stitutional Review Boards of the National Research Institute for Child Health and Development, the National Institute of Infectious Diseases, and the Tokyo Cord Blood Bank.

Preparation of EBV inocula and their titration, intravenous inoculation to humanized NOG mice, and quantification of viral DNA were performed as described elsewhere [6]. In brief, virus production from Akata cells was stimulated by treatment with anti-IgG antibody (DAKO), and culture fluid was used as inoculum after filtration through a 0.45-μm membrane filter. EBV titers in TD_{50} were determined by the Reed-Muench method.

In T cell reduction experiments, humanized NOG mice were inoculated with EBV at a dose of 1×10^2 TD_{50}. Starting at 21 days after inoculation, the Orthoclone OKT3 antibody specific to CD3 (Janssen Pharmaceutical) or the B9.11 antibody specific to CD8 (Beckman-Coulter) was administered intravenously at a dosage of 2 μg/mouse/day everyday until the end of the experiment. In a typical mouse treated with OKT3, 0.1% of human $CD45^+$ cells were $CD4^+CD8^-$ and 0.8% were $CD4^-CD8^+$ 2 weeks after the initiation of OKT3 administration, whereas in a control mouse, 15.0% of human $CD45^+$ cells were $CD4^+CD8^-$ and 12.5% were $CD4^-CD8^+$. Thus, this antibody was effective in significantly reducing the number of specific target cells. Confirmation of the reduction of $CD8^+$ cells by B9.11 was not possible, because this antibody covered the epitope recognized by antibodies available for flow cytometry. Survival curves of antibody-treated and untreated mice were compared statistically by the log-rank test.

Direct suppression of EBV-induced B cell transformation by $CD8^+$ T cells was assessed by the transformation regression assay based on a previously described method [11, 12]. $CD8^+$ T cells were isolated, as described elsewhere [6], from the spleen of EBV-infected or uninfected humanized NOG mice. Mononuclear cells were isolated from the spleen of uninfected humanized NOG mice and were inoculated with EBV (3×10^3 TD_{50} per 1×10^7 splenocytes). These EBV-infected cells were dispensed into microplates (3×10^4–1×10^5 cells/well) and were mixed with $CD8^+$ T cells.in the wells of microculture plates at different ratios. Half of the medium was replaced with fresh medium each week, and the outgrowth of lymphoblastoid cell lines was counted 8 weeks after initiation of the culture. Humanized NOG mice in the same lot were used in each experiment to attain common background of human major histocompatibility complex. The number of $CD8^+$ T cells required to achieve regression in 50% of the wells (50% regression dose) was calculated by the Reed-Muench method.

Results. Our previous experiments indicated that EBV-infected humanized NOG mice mount an EBV-specific T cell response that may be involved in immunological control of EBV. A time course of the levels of EBV DNA and $CD8^+$ T cells in the peripheral blood of a representative EBV-infected mouse (Figure 1*A*) suggested that these parameters change in an associated manner; there was a tendency for $CD8^+$ T cells to increase after surges in the EBV DNA level and to gradually decrease as the EBV DNA level decreased, suggesting that these $CD8^+$ T cells have some role in the control of EBV DNA level.

Table 1. Fifty Percent Regression Dose of $CD8^+$ T Cells in Epstein-Barr Virus (EBV)–Infected and Uninfected Mice

	50% Regression dose	
Experiment[a]	EBV-infected mice	Uninfected mice
A1	2.7×10^4	$>9.9 \times 10^4$
B1-1	2.7×10^5	$>1.4 \times 10^6$
B1-2	2.4×10^5	$>8.5 \times 10^5$
B2	1.1×10^5	$>4.2 \times 10^5$
B3[b]	$>2.3 \times 10^5$	$>3.0 \times 10^5$
C1[b]	$>3.9 \times 10^5$	$>3.2 \times 10^5$
C2	2.0×10^4	$>1.7 \times 10^6$

[a] Alphabetical letters signify the lot of a mouse, and the number immediately after the letter indicates an individual mouse. Numbers after a hyphen identify individual experiments.

[b] No significant regression was seen in these experiments.

To examine the protective role of T cells more precisely, we next tested whether the development of T cells has any influence on the mice's resistance to EBV infection. After transplantation with human HSCs, B cells develop first, ~3 months after transplantation, and T cells differentiate later, ~6 months after transplantation [10]. We divided 12 humanized NOG mice in a lot into 2 groups; 6 mice were inoculated with EBV (1×10^3 TD_{50}) at 96 days after transplantation with HSCs, and the remaining 6 were inoculated at 194 days. Mice were examined daily, and those exhibiting signs of severe illness, including weight loss, piloerection, and cachexia, were sacrificed for analysis. On autopsy, most of these mice showed the signs of lymphoproliferative disorder, as described elsewhere [6]. Figure 1*B* shows the survival curve of each group of infected mice, and the log-rank test indicated that the mice inoculated at 6 months after transplantation (ie, with fully developed T cells) had a significantly elongated life span ($P < .001$).

Because the aforementioned results suggested that T lymphocytes reconstituted in humanized NOG mice have some role in the protection against EBV-induced lymphoproliferative disorder, we then examined the effect of the anti-CD3 monoclonal antibody OKT3, which can deplete T cells in vivo [13]. Eighteen humanized NOG mice inoculated with 1×10^2 TD_{50} EBV were divided into 2 groups; 10 mice were given OKT3 beginning at 21 days after inoculation, and the remaining 8 were not given the antibody. Figure 1*C* shows the survival curve of these mice. The log-rank test indicated that those mice treated with OKT3 antibody had a significantly shorter life span, compared with control mice ($P < .01$). Similar OKT3 treatment

was performed with 7 humanized NOG mice that were not infected with EBV; 4 mice were given OKT3 antibody, and 3 were not. The result indicated that all mice in both groups survived the observation period of 150 days, and no difference could be seen between them, excluding the possibility that OKT3 has its own toxicity (Figure 1*C*). In accordance with this result, quantification with real-time polymerase chain reaction indicated that the level of EBV DNA in the peripheral blood was consistently higher in the OKT3-treated mice than in control mice (Figure 1*D*). Because $CD8^+$ cytotoxic T cells are considered to play a central role in the immune response to EBV, we next examined the effect of an antibody (B9.11) specific to the CD8 molecule [14]. Figure 1*E* shows the survival curves of EBV-infected humanized NOG mice that were either treated with B9.11 or not, and the log-rank test indicated that those mice treated with the antibody had a significantly reduced life span after EBV infection ($P < .05$).

To test whether T cells isolated from EBV-infected mice have the ability to suppress transformation of autologous B cells by EBV, we used the transformation regression assay. Mononuclear cells isolated from the spleen of humanized NOG mice were inoculated with EBV and were cocultured with $CD8^+$ T cells isolated from the spleen of either EBV-infected or uninfected mice. Table 1 shows the number of $CD8^+$ T cells required to inhibit the outgrowth of EBV-infected cells in 50% of the wells (50% regression dose). These data indicate that $CD8^+$ T cells isolated from EBV-infected mice, but not those from uninfected mice, could suppress the outgrowth of transformed lymphoblastoid cell line.

Discussion. Humanized mouse technology has been successfully used to reproduce human immune responses to certain viruses that cannot infect ordinary mice [6–8, 10]. However, these studies have yet to provide evidence that immune responses induced in these mice are actually involved in the control of viral infections. This was an important issue when we considered the possibility of using humanized mice as a tool to evaluate immunological therapies and prophylaxes to viral infections.

Humanized NOG mice in later stages of reconstitution that contained high numbers of T cells had significantly longer life spans after EBV infection, compared with those in earlier stages that lacked significant differentiation of T cells. In accordance with this result, treatment of EBV-infected humanized NOG mice with OKT3, which can deplete $CD3^+$ T cells, significantly reduced their life span. Furthermore, similar antibody-mediated reduction in the number of $CD8^+$ T cells also reduced the life span of infected humanized NOG mice. Thus, our results strongly suggest that human T cells that develop in humanized NOG mice contribute to their resistance to EBV infection. More-direct evidence of immunological control of EBV infection was obtained by the transformation regression assay, which has been used as one of the most reliable methods to quantify EBV-specific cytotoxic T cells. This assay clearly indicated that $CD8^+$ T cells isolated from EBV-infected mice can suppress EBV-induced transformation of autologous B cells. A study is underway to identify an epitope that can be recognized by a $CD8^+$ T cell clone.

To our knowledge, these results are the first evidence that immune responses induced in humanized mice are actually involved in an effective control of viral infection. It is thus suggested that the NOG mouse model of EBV infection is a useful tool to evaluate candidate vaccines and immunological therapies for EBV infection.

After the initial submission of this report, Strowig and others published a work containing similar findings, namely higher EBV load and lymphoproliferative disorder in humanized mice after T cell depletion [15].

Acknowledgments

We thank Motohiko Okano, for advice in regression assay; Miki Mizukami, Ken Watanabe, and Miki Katayama, for technical assistance; Yuko Tatsumi and Tomomi Hakuya, for secretarial assistance; and Tokyo Cord Blood Bank, for supplying cord blood.

References

1. Rickinson AB, Kieff E. Epstein-Barr virus. In: Knipe DM, Howley PM, eds. Fields virology. 5th ed. Vol. 2. Philadelphia: Lippincott Williams & Wilkins, **2007**:2655–700.
2. Kieff E, Rickinson AB. Epstein-Barr virus and its replication. In: Knipe DM, ed. Fields virology. 5th. ed. Vol. 2. Philadelphia: Lippincott Williams & Wilkins, **2007**:2603–54.
3. Hislop AD, Taylor GS, Sauce D, Rickinson AB. Cellular responses to viral infection in humans: lessons from Epstein-Barr virus. Annu Rev Immunol **2007**; 25:587–617.
4. Babcock GJ, Decker LL, Volk M, Thorley-Lawson DA. EBV persistence in memory B cells in vivo. Immunity **1998**; 9:395–404.
5. Ito M, Hiramatsu H, Kobayashi K, et al. NOD/SCID/gamma(c)(null) mouse: an excellent recipient mouse model for engraftment of human cells. Blood **2002**; 100:3175–82.
6. Yajima M, Imadome KI, Nakagawa A, et al. A new humanized mouse model of Epstein-Barr virus infection that reproduces persistent infection, lymphoproliferative disorder, and cell-mediated and humoral immune responses. J Infect Dis **2008**; 198:673–82.
7. Melkus MW, Estes JD, Padgett-Thomas A, et al. Humanized mice mount specific adaptive and innate immune responses to EBV and TSST-1. Nat Med **2006**; 12:1316–22.
8. Traggiai E, Chicha L, Mazzucchelli L, et al. Development of a human adaptive immune system in cord blood cell-transplanted mice. Science **2004**; 304:104–7.
9. Watanabe S, Ohta S, Yajima M, et al. Humanized NOD/SCID/IL2Rgamma(null) mice transplanted with hematopoietic stem cells under nonmyeloablative condition show prolonged lifespans and allow detailed analysis of human immunodeficiency virus type 1 pathogenesis. J Virol **2007**; 81:13259–64.
10. Watanabe S, Terashima K, Ohta S, et al. Hematopoietic stem cell-engrafted NOD/SCID/IL2Rgamma null mice develop human lymphoid

systems and induce long-lasting HIV-1 infection with specific humoral immune responses. Blood **2007**; 109:212–8.
11. Moss DJ, Rickinson AB, Pope JH. Long-term T-cell-mediated immunity to Epstein-Barr virus in man. I. Complete regression of virus-induced transformation in cultures of seropositive donor leukocytes. Int J Cancer **1978**; 22:662–8.
12. Okano M, Purtilo DT. Simple assay for evaluation of Epstein-Barr virus specific cytotoxic T lymphocytes. J Immunol Methods **1995**; 184:149–52.
13. Dessureault S, Shpitz B, Alloo J, et al. Physiologic human T-cell responses to OKT3 in the human peripheral blood lymphocyte-severe combined immunodeficiency mouse model. Transplantation **1997**; 64: 811–6.
14. Kobayashi E, Kawai K, Ikarashi Y, Fujiwara M. Mechanism of the rejection of major histocompatibility complex class I-disparate murine skin grafts: rejection can be mediated by CD4+ cells activated by allo-class I + II antigen in CD8+ cell-depleted hosts. J Exp Med **1992**; 176: 617–21.
15. Strowig T, Gurer C, Ploss A, et al. Priming of protective T cell responses against virus-induced tumors in mice with human immune system components. J Exp Med **2009**; 206:1423–34.

Epstein–Barr virus-encoded latent membrane protein 1 activates β-catenin signaling in B lymphocytes

Mariko Tomita,[1] Md. Zahidunnabi Dewan,[2,3,5] Naoki Yamamoto,[2,3] Akira Kikuchi[4] and Naoki Mori[1,6]

[1]Division of Molecular Virology and Oncology, Graduate School of Medicine, University of the Ryukyus, Okinawa; [2]Department of Molecular Virology, Graduate School, Tokyo Medical and Dental University, Tokyo; [3]AIDS Research Center, National Institute of Infectious Disease, Tokyo; [4]Department of Biochemistry, Graduate School of Biomedical Science, Hiroshima University, Hiroshima, Japan

(Received November 28, 2008/Revised January 4, 2009/Accepted January 21, 2009/Online publication March 20, 2009)

The Epstein–Barr virus-encoded latent membrane protein 1 is considered the Epstein–Barr virus oncogene based on its importance in Epstein–Barr virus-induced B-lymphocyte transformation. β-Catenin is a potential oncogene, and its accumulation has been implicated in a variety of human cancers. Here, we found that β-catenin protein was highly expressed in Epstein–Barr virus-immortalized B-cell lines compared with peripheral blood mononuclear cells from healthy donors. β-Catenin expression in Epstein–Barr virus-immortalized B-cell line decreased following treatment with LY294002, an inhibitor of phosphatidylinositol 3-kinase. Treatment with LY294002 or knockdown of β-catenin by small interfering RNA reduced the growth of Epstein–Barr virus-immortalized B-cell line. Transient transfection of latent membrane protein 1 expression plasmid increased β-catenin protein expression and β-catenin-dependent transcription. Latent membrane protein 1 deletions mutants lacking the carboxyl-terminal activating region 1 domain failed to enhance β-catenin protein expression and β-catenin-dependent transcriptional activity. They also failed to increase phosphorylated AKT expression. Dominant-negative AKT suppressed latent membrane protein 1-induced β-catenin-dependent transcriptional activity. These results suggest that latent membrane protein 1 activates β-catenin through the phosphatidylinositol 3-kinase/AKT signaling pathway. Activation of the β-catenin pathway by Epstein–Barr virus may contribute to the lymphoproliferation characteristic of Epstein–Barr virus-infected B-cells. (*Cancer Sci* 2009; 100: 807–812)

Epstein–Barr virus (EBV), a member of the herpes virus family, has been identified as the first human tumor virus associated with several malignancies. Cancers linked to EBV include lymphomas that develop in the immunocompromised individuals, Hodgkin's disease, Burkitt's lymphoma, and nasopharyngeal carcinoma.[1] Regardless of their type, the majority of tumor cells are latently infected with EBV. LMP1, a viral latency protein, is considered an EBV oncogene based on its importance in EBV-induced B-lymphocyte transformation.[2] LMP1 is an integral membrane protein consisting of 386 amino acids that form a short amino-terminal cytoplasmic end, six hydrophobic transmembrane domains, and a long carboxyl-terminal tail that contains the two main signaling domains, CTAR-1 and -2.[3] Through self clustering in the membrane, LMP1 acts as a constitutively active TNF receptor and mimics many of the phenotypic consequences of TNF receptor family such as TNF receptor and CD40 activation. CTAR-1 interacts with members of the TRAF family, TRAF1 and TRAF2, and induces NF-κB signaling.[4,5] CTAR-2 associates with TRADD protein and also mediates NF-κB signaling.[6] CTAR-2 also induces the activity of AP-1 transcription factor via signaling pathway that involves c-Jun N-terminal kinase.[7,8] LMP1 also activates p38 MAPK through both CTAR-1 and CTAR-2.[9] In addition, LMP1 activates the p44/p42 MAPK[10] and JAK/STAT[11] pathways.

Phosphatidylinositol 3-kinase (PI3K)/AKT signaling is often activated in many human cancer cells.[12] It is activated by a wide range of extracellular growth and mitogenic stimuli including ligands of the TNF receptor family, thus suggesting that LMP1 may also target this pathway. Indeed, previous studies have shown that LMP1 can activate the PI3K/AKT pathway.[13,14] CTAR-1 activates PI3K/AKT signaling, resulting in the phosphorylation of the AKT target, GSK3β. The activation of PI3K/AKT is responsible for LMP1-induced actin polymerization and transformation, and also contributes to cell survival.[13,14]

The Wnt/β-catenin signaling cascade is an important pathway activated in various cancers. β-Catenin is a critical component of the Wnt signaling pathway.[15] Stabilized or free β-catenin can translocate to the nucleus and bind transcription factors, such as the Tcf or Lef, to activate transcription. β-Catenin-Tcf/Lef complexes regulate a number of protooncogenes, including *c-myc* and *cyclin D1*. Previous studies have shown that β-catenin is a potential oncogene,[16] and its accumulation has been implicated in a variety of human cancer cells.[17]

We reported previously that HTLV-1, the causative agent of ATL, induces β-catenin protein accumulation and transcriptional activation via the PI3K/AKT signaling pathway.[18] LMP1 also activates PI3K/AKT pathway;[13,14] however, the role of LMP1 in β-catenin regulation through this signaling pathway in B lymphocytes has not yet been established. In this study, we determined whether the LMP1-mediated effects on PI3K/AKT signaling modulated β-catenin expression in EBV-infected B cells.

Materials and Methods

Reagents. PI3K inhibitor LY294002 and the MEK1/2 inhibitor PD98059 were purchased from Calbiochem (La Jolla, CA, USA).

Antibodies. We used primary antibodies against β-catenin (BD Transduction Laboratories, San Jose, CA, USA), LMP1 (CS.1–4) (Dako, Glostrup, Denmark), actin (Lab Vision, Fremont, CA, USA), phospho-AKT (Ser473), AKT, phospho-p44/p42 MAPK (Erk1/2) (Thr202/Tyr204), and p44/p42 MAPK (Erk1/2) (Cell Signaling Technology, Beverly, MA, USA). Horseradish-peroxidase-conjugated secondary antibodies were purchased from GE Healthcare (Waukesha, WI, USA).

Cell lines. EBV-immortalized LCLs (LCL-Ao, LCL-Ka, and LCL-Ku) were established by infection of lymphocytes from three healthy donors with culture supernatants of the virus producer

[5]Present address: Department of Pathology, New York University School of Medicine, New York, USA.
[6]To whom correspondence should be addressed. E-mail: n-mori@med.u-ryukyu.ac.jp

Abbreviations: ATL, adult T-cell leukemia; CTAR, carboxyl-terminal activating region; EBV, Epstein-Barr virus; GSK3β, glycogen synthase kinase 3β; HTLV-1, human T-cell leukemia virus type 1; JAK/STAT, janus kinase/signal transducers and activators of transcription; LCLs, lymphoblastoid cell lines; Lef, lymphocyte enhancer factor; LMP, latent membrane protein; MAPK, mitogen-activated protein kinase; MEK1/2, mitogen-activated protein/extracellular signal-regulated kinase; MTT, 3-(4,5-Dimethyl-2-thiazolyl)-2,5-diphenyl-2*H*-tetrazolium bromide; NF-κB, nuclear factor-kappaB; PI3K, phosphatidylinositol 3-kinase; PBMC, peripheral blood mononuclear cells; SDS-PAGE, sodium dodecyl sulfate–polyacrylamide gel electrophoresis; siRNA, small interfering RNA; Tcf, T-cell factor; TK, tymidine kinase; TNF, tumor necrosis factor; TRADD, TNF receptor-associated death domain protein; TRAF, TNF receptor-associated factor; WST-8, 2-(2-methoxy-4-nitrophenyl)-3(4-nitrophenyl)-5-(2,4-disulfophenyl)-2*h* tetrazolium monosodium salt.

doi: 10.1111/j.1349-7006.2009.01121.x

B95.8 line as described previously,[19] and cultured in RPMI-1640 medium supplemented with 10% heat-inactivated fetal bovine serum, 50 U/mL penicillin, and 50 μg/mL streptomycin at 37°C in 5% CO_2. HeLa cells (human cervix adenocarcinoma cell line) were maintained in Dulbecco's modified Eagle's medium supplemented with 10% heat-inactivated fetal bovine serum, 50 U/mL penicillin, and 50 μg/mL streptomycin at 37°C in 5% CO_2.

Peripheral blood mononuclear cells (PBMCs). PBMCs from healthy volunteers were isolated by Ficoll-Paque density gradient centrifugation (GE Healthcare). All blood samples were obtained after informed consent.

Western blot analysis. Western blot analysis was performed as described previously.[20] In brief, whole cell lysates were subjected to SDS-PAGE, electroblotted onto polyvinylidene difluoride membranes (Millipore, Billerica, MA, USA) and then analyzed for immunoreactivity with the appropriate primary and secondary antibodies as indicated in the figures. Reaction products were visualized using Enhanced Chemiluminescence reagent, according to the instructions provided by the manufacturer (Amersham Pharmacia, Uppsala, Sweden).

Cellular proliferation assay. Proliferation of LCL-Ka cells after treatment with LY294002 or PD98059 was analyzed by counting viable cells using the Trypan blue exclusion method. The antiproliferative effects of LY294002 against LCL-Ka and PBMCs from a healthy donor were measured by the WST-8 method (Cell Counting Kit-8; Wako Pure Chemical Industries, Osaka, Japan) based on the MTT assay, as described previously.[21] Briefly, the 5×10^3 cells were incubated in triplicate in a 96-well microculture plate in the presence of different concentrations of LY294002 (0–50 μM) in a final volume of 0.1 mL for 48 h at 37°C. Thereafter, 5-μL Cell Counting Kit-8 solution (5 mM WST-8, 0.2 mM 1-methoxy 5-methylphenazinium methylsulfate, and 150 mM NaCl) was added, and the cells were further incubated for another 4 h. The number of surviving cells was measured by a 96-well multiscanner autoreader at optical density of 450 nm. Cell viability was determined as percentage of the control (absence of LY294002).

Small interfering RNA (siRNA). To repress β-catenin, a predesigned double-stranded siRNA (siGENOME SMARTpool CTNNB1; Dharmacon, Lafayette, CO, USA) was used. A siCONTROL nontargeting siRNA pool (Dharmacon) was used as a negative control. siRNA was transfected into LCL-Ka cells at 100 nM of the final concentration. The transfected cells were incubated for 12 h, seeded into 24-well plates at 5×10^4 viable cells per well, and incubated for the indicated time periods. The number of viable cells was determined every 24 h by counting Trypan blue excluding cells in a hemocytometer.

Plasmids. The β-catenin expression plasmid (pCGN/β-catenin) and human Tcf-4 expression plasmid (pEF-BOS HA/Tcf-4E) have been described previously.[22,23] The pGL3-OT and pGL3-OF reporter plasmids[24] were kindly provided by Dr B. Vogelstein (Sidney Kimmel Comprehensive Cancer Center, Johns Hopkins University School of Medicine, Baltimore, MD, USA). pGL3-OT and pGL3-OF contain three copies of the Tcf site (5′-AGATCAA AGG-3′) and a mutant sequence (5′-AGGCCAAAGG-3′), respectively, upstream of the c-*fos* promoter and the luciferase open reading frame. The expression plasmids pSG5-LMP1, pSG5-LMP1Δ187-351, pSG5-LMP1349Δ, and pSG5-LMP1Δ194-386 were provided by Dr M. Rowe (University of Wales College of Medicine, Cardiff, UK).[25,26] The dominant-negative AKT expression plasmid (pCMV5-K169A, T308A, S473A-AKT) had Lys-169-, Thr-308-, and Ser-473-to-Ala mutations and was kindly provided by Dr D. Alessi (University of Dundee, Dundee, UK).

Transfection. HeLa cells were transfected using Lipofectamine reagent (Invitrogen, Carlsbad, CA, USA) according to the protocol supplied by the manufacturer. LCL-Ka cells were transfected by using MicroPorator MP-100 (Digital Bio Technology, Seoul, Korea) according to the instructions supplied by the manufacturer for optimization and use.

Luciferase assay. Cells were transiently transfected with the indicated effecter plasmids and a luciferase reporter construct. In all cases, the reference plasmid phRL-TK (Promega, Madison, WI, USA), which contains the *Renilla* luciferase gene under the control of the TK promoter, was cotransfected to correct for transfection efficiency. Luciferase assays were performed by using the Dual-Luciferase Reporter System (Promega), in which relative luciferase activities were calculated by normalizing transfection efficiency according to the *Renilla* luciferase activities.

Statistical analysis. Data of cell proliferation assay were expressed as mean ± SD. Differences between groups were examined for statistical significance by the unpaired Student's *t*-test. A *P*-value less than 0.05 denoted the presence of a statistically significant difference.

Results

β-Catenin protein is highly expressed in EBV-immortalized B-cells and correlates with LMP1 expression and AKT phosphorylation. First, we analyzed protein expression of β-catenin in EBV-immortalized B-cell lines. β-Catenin protein was highly expressed in EBV-immortalized B-cell lines compared with normal PBMCs (Fig. 1a). Although the expression of β-catenin was higher in LCLs than in normal PBMCs, β-catenin expression level varied among EBV-immortalized B-cell lines (highest expression in LCL-Ka and lowest expression in LCL-Ao). To determine whether AKT activity is associated with β-catenin expression in EBV-infected cells, we examined the phosphorylation status of AKT relative to β-catenin protein expression in EBV-immortalized B-cell lines (Fig. 1a). Phosphorylated AKT and β-catenin were detected in all EBV-immortalized B-cell lines, and the expression levels of these proteins were similar to those of LMP1 in these cells.

PI3K/AKT signaling contributes to β-catenin expression and EBV-immortalized B-cell growth. Next, to determine the role of PI3K/AKT signaling in the expression of β-catenin in EBV-immortalized B-cell lines, LCL-Ka cells, which expressed the highest levels of β-catenin, LMP1, and phosphorylated AKT proteins among EBV-immortalized B-cell lines, were treated with the PI3K inhibitor LY294002 (Fig. 1b). β-Catenin expression was significantly reduced in the presence of LY294002. Phosphorylation of AKT was also inhibited by LY290042, whereas the total level of AKT was unaffected. Treatment with LY294002 did not change the expression of LMP1. On the other hand, MEK1/2 inhibitor PD98059 did not change both β-catenin and phosphorylated AKT protein levels, although it decreased the level of phosphorylated p44/p42 MAPK.

To elucidate the effect of PI3K/AKT signaling on the growth of EBV-immortalized B cells, LCL-Ka cells were first treated with either PD98059 or LY294002, followed by counting the cell numbers at 1, 2, and 3 days (Fig. 1c, left panel). The growth of LCL-Ka cells were suppressed by both PD98059 and LY294002 treatments. However, the effect of LY294002 was greater than that of PD98059. To verify the specificity of LY294002 and rule out nonspecific toxicity of this drug, we also analyzed the effect of LY294002 on the viability of PBMCs from a healthy donor, whose PI3K/AKT signaling pathway was not activated. The result of these analyses demonstrated that inhibition of PI3K/AKT signaling pathway by LY294002 did not suppress cell viability of PBMCs from a healthy donor (Fig. 1c, right panel), indicating that the effects of LY294002 on LCL-Ka were not non-specific toxicity of this drug. We also found that knockdown of β-catenin by siRNA inhibited the growth of LCL-Ka cells (Fig. 1d, left panel). The efficiency of knockdown was moderate (Fig. 1d, right panel) due to the low transfection efficiency (40–50%) of these cells (data not shown).

LMP1 induces expression and transcriptional responses of β-catenin. Next, we examined the role of LMP1 in the expression of β-catenin. β-Catenin protein expression was induced by transient transfection of LMP1 expression plasmids (Fig. 2a). We next examined whether the induction of β-catenin by LMP1 affected

doi: 10.1111/j.1349-7006.2009.01121.x

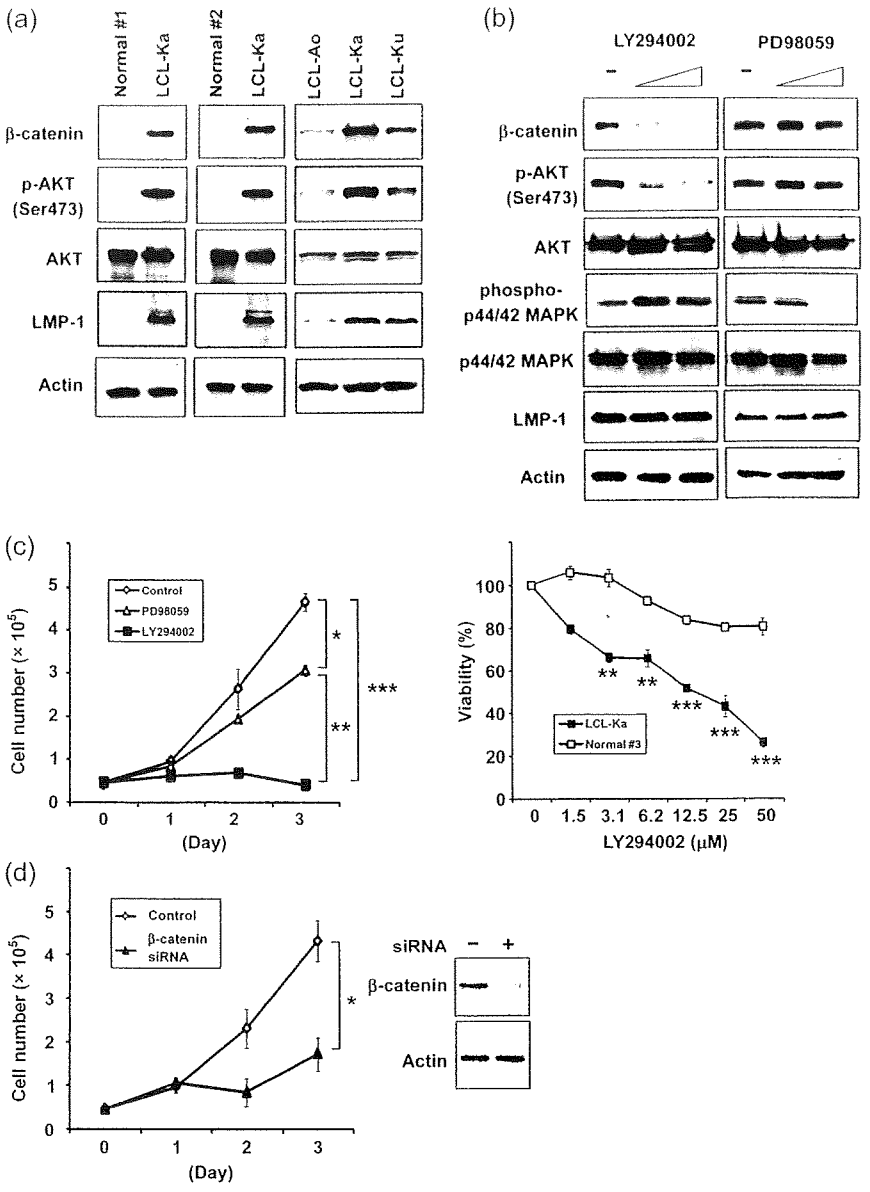

Fig. 1. Inhibition of phosphatidylinositol 3-kinase (PI3K)/AKT reduced β-catenin expression and cell growth of Epstein–Barr vius (EBV)-immortalized B-cell lines. (a) Total cell lysates of EBV-immortalized B-cell lines (lymphoblastoid cel lines [LCL]-Ao, LCL-Ka, and LCL-Ku) and normal peripheral blood mononuclear cells (PBMCs) (Normal #1 and #2) were resolved in sodium dodecyl sulfate–polyacrylamide gel electrophoresis (SDS-PAGE) and probed with anti-β-catenin, antiphospho-AKT (Ser473), anti-AKT, and anti-latent membrane protein 1 (LMP1) antibodies. Actin was the loading control. (b) LCL-Ka cells were treated with increasing amounts (0, 25, and 50 μM) of PI3K inhibitor LY294002 or mitogen-activated protein/extracellular signal-regulated kinase inhibitor PD98059 for 48 h. Total cell lysates were resolved in SDS-PAGE and probed with anti-β-catenin, antiphospho-AKT (Ser473), anti-AKT, antiphospho p44/p42 mitogen-activated protein kinase (MAPK), antip44/p42 MAPK, and anti-LMP1 antibodies. Actin was the loading control. Representative results of three experiments with similar findings. (c) PI3K inhibitor LY294002 suppressed the growth of EBV-immortalized B-cell line. LCL-Ka cells (5×10^4 cells/mL) were treated with 50 μM of either LY294002 or PD98059, or vehicle (control) for the indicated time periods. Viable cell numbers were counted in triplicate by Trypan blue dye exclusion method. Data are mean ± SD of three separate experiments ($^*P < 0.01$, $^{**}P < 0.001$ and $^{***}P < 0.0005$) (left panel). LCL-Ka cells and PBMCs from a healthy donor (Normal #3) were treated with increasing amount of LY294002 (0–50 μM) for 48 h. Cell viability was assessed by the 2-(2-methoxy-4-nitrophenyl)-3(4-nitrophenyl)-5-(2,4-disulfophenyl)-*2h* tetrazolium monosodium salt (WST-8) method. Data are expressed as the mean ± SD percentage of the control (untreated cells). Significance of differences between percentage viable cells of LY294002 treated cells and that of untreated cells are shown as *P*-values ($^{**}P < 0.001$ and $^{***}P < 0.0005$) (right panel). (d) Knockdown of β-catenin suppressed the growth of EBV-immortalized B-cell line. LCL-Ka cells were transfected with siRNA for β-catenin or with a non-target siRNA (final concentration of siRNA was 100 nM). The effect of knockdown of β-catenin on cell growth was examined by counting the number of viable cells in triplicate using the trypan blue dye-exclusion method (left panel). Data are mean ± SD of three separate experiments ($^*P < 0.05$). Western blotting analysis showing repression of β-catenin in LCL-Ka cells transfected with β-catenin siRNA (+) compared with that in cells transfected with non-targeting siRNA (–) (right panel). Cells were collected 48 h after transfection. Actin was the loading control. Representative results of three experiments with similar findings.

β-catenin/Tcf transcriptional activity (Fig. 2b). In a transient transfection reporter assay using pGL3-OT as a reporter, the expression of LMP1 alone in HeLa cells activated the reporter activity. The combination of β-catenin and LMP1 had an even greater effect. No significant responses were seen with the mutant reporter (pGL3-OF) (data not shown).

CTAR-1 is required for activation of β-catenin by LMP1. To identify the domain within the LMP1 cytoplasmic tail responsible for the induction of the transcriptional activity of β-catenin/Tcf, reporter assay was performed with LMP1 mutants defective for the CTAR-1 and CTAR-2 effecter domains (Fig. 3b). Figure 3(a) (left panel) shows schematic diagrams of the wild type and mutants of LMP1 expression plasmids. HeLa cells transfected with either the wild-type or mutants LMP1 expression plasmids expressed comparable levels of LMP1 protein as determined by western blotting (Fig. 3a, right panel). The LMP1 CTAR-1/CTAR-2 double mutant Δ194-386 was not detected by CS. 1–4 antibodies since it lacks the epitopes recognized by these antibodies. Expression of the CTAR-1 mutant Δ187-351 showed little induction of reporter activation, implicating CTAR-1 as the domain of LMP1 responsible for this response. This was confirmed with the CTAR-2 mutant 349Δ, where the expression resulted in activation of the reporter, similar to the wild-type LMP1. The CTAR-1/CTAR-2 double mutant Δ194-386 failed to induce reporter activation, consistent with the role of CTAR-1 in this effect. Next, we analyzed the effect of CTAR-1 on the induction of β-catenin protein expression (Fig. 3c). Transient transfection of either the wild-type or mutant LMP1 expression plasmids in HeLa cells showed that CTAR-1 mutant Δ187-351 and CTAR-1/CTAR-2 double mutant Δ194-386 had little effects on the induction of β-catenin protein than wild-type and CTAR-2 mutant 349Δ.

Activation of β-catenin by LMP1 is associated with AKT activity. Activation of AKT signaling is associated with accumulation of β-catenin.[27] To determine whether AKT activation is associated

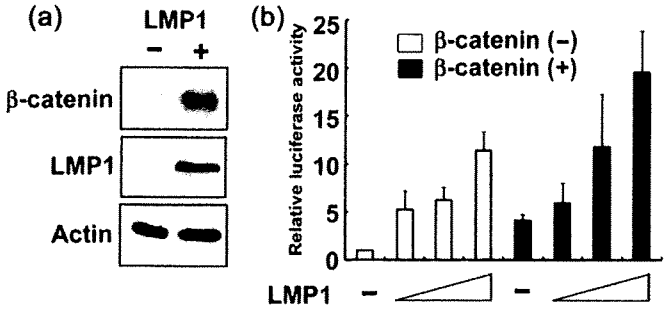

Fig. 2. Latent membrane protein 1 (LMP1) induced expression and transcriptional responses of β-catenin. (a) LMP1 induced expression of β-catenin protein. HeLa cells were transfected with either 2 μg of LMP1 expression plasmid (+) or empty vector (–). Cells were collected 48 h after transfection. Total cell extracts from transfected HeLa cells were analyzed for β-catenin and LMP1 protein expression by western blot analysis. Actin was a loading control. Representative results of three experiments with similar findings. (b) Transient expression assay evaluating the activity of β-catenin/T-cell factor (Tcf)-regulated reporter. HeLa cells were transfected with the pGL3-OT reporter (2 μg), Tcf (0.1 μg), and either LMP1 (0, 0.5, 1, or 2 μg) or β-catenin (0.5 μg) plus LMP1. Cells were collected 48 h after transfection. Data are mean ± SD of triplicate experiments.

with LMP1-induced β-catenin activity, we examined the phosphorylation status of AKT in HeLa cells transiently transfected with either wild-type or mutant LMP1 expression plasmids (Fig. 3c). CTAR-1 mutant Δ187-351 and CTAR-1/CTAR-2 double mutant Δ194-386 had less important effects on the phosphorylation of AKT than wild-type and CTAR-2 mutant 349Δ. These results indicate that LMP1 activates AKT through CTAR-1 cytoplasmic tail.

Dominant-negative AKT suppresses LMP1-induced β-catenin/Tcf transcriptional activity. To determine the role of AKT in the LMP1-induced β-catenin/Tcf transcriptional activity, we used the dominant-negative mutant AKT expression plasmid, AKT-DN, to directly examine the role of AKT in LMP1-induced β-catenin/Tcf transcription (Fig. 3d). AKT-DN suppressed the LMP1-induced pGL3-OT activity. pGL-OF activity was not affected by AKT-DN plasmid (data not shown).

Discussion

EBV-positive malignancies in immunocompromised patients are associated with high mortality and reduced overall survival period. Here, we demonstrated the important roles of β-catenin in the growth of EBV-immortalized B-cell lines and the role of LMP1 in activation of β-catenin in these cells. We found that EBV-immortalized B cell lines highly expressed β-catenin protein compared with normal PBMCs. Knockdown of β-catenin by siRNA reduced the growth of LCL-Ka cells, indicating that β-catenin plays an important role in the growth of EBV-immortalized B cell lines. EBV transforming protein LMP1 induced β-catenin protein expression and transcriptional activity. β-Catenin protein levels in LCL-Ka cells were reduced by treatment with PI3K inhibitor LY294002. In this regard, a recent study has shown that LMP1 regulates epithelial cell motility and invasion via the ERK/MAPK pathway.[28] We also found that MEK1/2 inhibitor, PD98059, suppressed the growth of LCL-Ka cells without decreasing β-catenin expression. However, the effect of PD98059 was less pronounced than that of LY294002, suggesting that β-catenin may have a dominant role in the growth of these cells. Moreover, dominant-negative AKT inhibited LMP1-induced β-catenin-dependent transcription. These results suggest that LMP1 activates β-catenin via the PI3K/AKT signaling pathway.

Previous studies reported that LMP1 activates PI3K/AKT signaling, resulting in enhancement of cell transformation and survival of epithelial cells.[13,14] Here, we showed that the same signaling

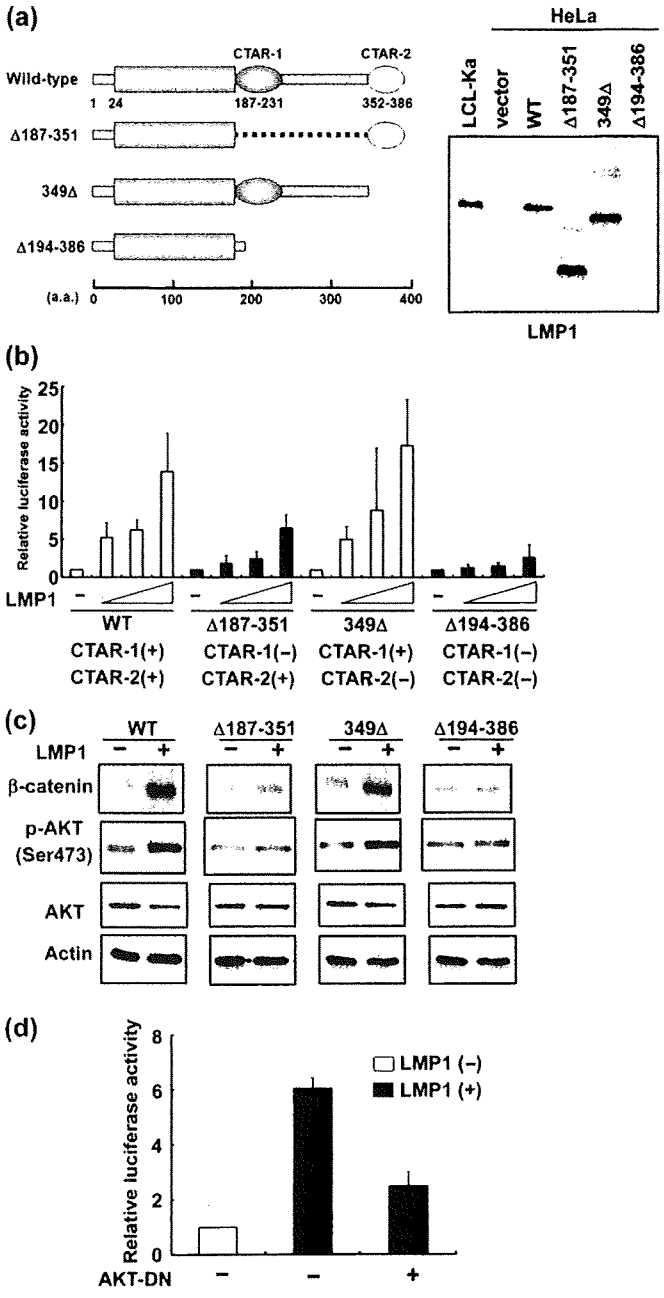

Fig. 3. Carboxyl-terminal activating region 1 (CTAR-1) is required for activation of β-catenin/T-cell factor (Tcf) transcription by latent membrane protein 1 (LMP1). (a) Schematic diagrams of wild-type (WT) and mutants LMP1 (left panel). HeLa cells were transfected with either wild-type or mutant LMP1 expression plasmids (right panel). Cells were collected 48 h after transfection and total lysates were analyzed for LMP1 expression by western blot analysis. (b) HeLa cells were transfected with the pGL3-OT reporter (2 μg), Tcf expression plasmid (0.1 μg), and either LMP1 wild-type or LMP1 mutants (Δ187-351, 349Δ, or Δ194-386) (0, 0.5, 1, or 2 μg). Cells were collected 48 h after transfection. Data are mean ± SD of triplicate experiments. (c) HeLa cells were transfected with either wild-type LMP1 or LMP1 mutants (Δ187-351, 349Δ, and Δ194-386) expression plasmids (2 μg). Cells were collected 48 h after transfection. Total cell extracts from transfected HeLa cells were analyzed for β-catenin expression levels and phosphorylation status of AKT by western blot analysis. Actin was a loading control. Representative results of three experiments with similar findings. (d) Dominant-negative AKT suppressed LMP1-induced β-catenin/Tcf transcription. HeLa cells were transfected with the pGL3-OT reporter (2 μg), Tcf (0.1 μg), and either LMP1 (0.5 μg) or LMP1 with dominant-negative AKT (AKT-DN) (0.1 μg) as indicated in the figure. Cells were collected 48 h after transfection. AKT-DN suppressed LMP1-induced β-catenin/Tcf transcription. Data are mean ± SD of triplicate experiments.

doi: 10.1111/j.1349-7006.2009.01121.x

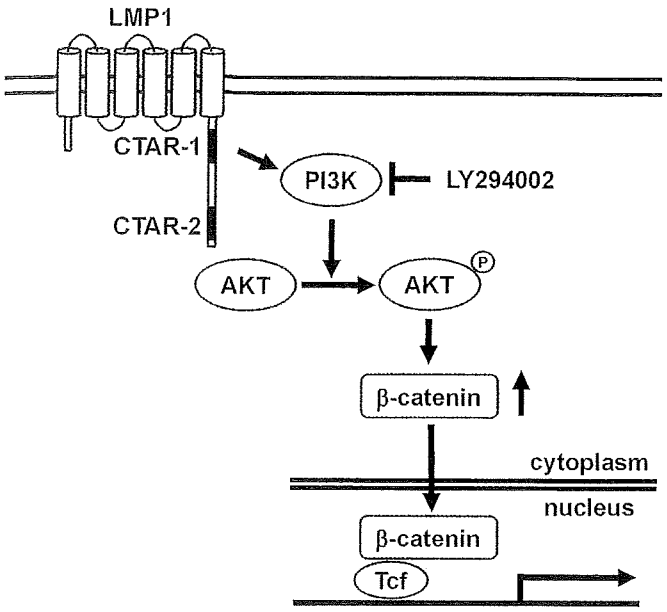

Fig. 4. Schematic representation of the effects of latent membrane protein 1 (LMP1) on the β-catenin signaling pathway. LMP1 activates phosphatidylinositol 3-kinase (PI3K)/AKT through carboxyl-terminal activating region 1 (CTAR-1) cytoplasmic tail. The activated AKT enhances β-catenin protein expression. Highly expressed β-catenin can translocate to the nucleus and bind to the transcription factor T-cell factor (Tcf).

is also important for the growth of EBV-immortalized B cells. They also demonstrated that the cytoplasmic COOH terminus of LMP1 is necessary for activation of PI3K/AKT signaling.[13] We confirmed these findings by showing that LMP1 mutants deficient in the CTAR-1 domain could not activate phosphorylation of AKT. LMP1 most closely resembles an activated CD40 in its phenotypic effects. In this regard, one study reported that CD40 ligation can activate PI3K/AKT signaling in B cells and that this effect is important for both cell proliferation and survival.[29] Furthermore, mice deficient in the p85 subunit of PI3K are severely impaired in B cell development with reduced proliferative responses to CD40 ligation.[30] Taken together, these data highlight the role of the PI3K/AKT signaling pathway in B cell growth and suggest that the ability of LMP1 to activate this pathway contributes to EBV persistence in B cells.

The Wnt/β-catenin signaling pathway has been identified as a common target for perturbation by viruses, as demonstrated by the following examples from the literature. HTLV-1 Tax, which activates PI3K/AKT signaling, results in GSK3β inactivation and β-catenin stabilization.[18] The latency-associated nuclear antigen of Kaposi's sarcoma-associated herpesvirus binds to GSK3β and sequesters it in the nucleus, preventing β-catenin phosphorylation.[31] Previously, Shackelford *et al.*[32] reported that β-catenin was activated in type III EBV-infected B lymphocytes. They found that β-catenin is associated with deubiquitination of enzymes.[32] Another EBV encoding LMP2A also activates PI3K/AKT signaling, resulting in GSK3β inactivation and β-catenin stabilization in epithelial cells.[33] It is not clear at present which LMP (LMP1 or LMP2A) is more important in activation of β-catenin in B lymphocytes. The roles of LMP2A in the growth of EBV-immortalized B cells are currently being investigated in our laboratory.

In summary, the data presented here show that β-catenin is activated in EBV-immortalized B-cells. β-Catenin signaling had an important role in the growth of EBV-immortalized B-cells. LMP1 activated β-catenin through PI3K/AKT signaling, and LMP1 CTAR-1 domain was crucial for activation of this pathway (Fig. 4). Our results implicate LMP1 in the activation of the β-catenin signaling pathway and hence in the malignant growth of B lymphocytes following EBV infection.

Acknowledgments

We thank Dr B. Vogelstein for providing reporter plasmids pGL3-OT and pGL3-OF, Dr M. Rowe for providing LMP1 and LMP1 mutant plasmids, and Dr D. Alessi for the dominant-negative AKT. We also thank all members of our laboratories for the helpful comments and collaborations. This work was supported in part by grants-in-aid from the Ministry of Education, Culture, Sports, Science and Technology of Japan (No. 19591122); Takeda Science Foundation; and Japan Leukemia Research Fund; and a grant from the Princes Takamatsu Cancer Research Fund (No. 07-23905) and Kanehara Ichiro Memorial Foundation for Promotion of Medicine.

References

1 Rickinson AB, Kieff E. Epstein-Barr virus and its replication. *Fields Virology*, 4th edn. Philadelphia, PA: Lippincott Williams & Wilkins, 2006: 2655–700.
2 Kaye KM, Izumi KM, Kieff E. Epstein-Barr virus latent membrane protein 1 is essential for B-lymphocyte growth transformation. *Proc Natl Acad Sci USA* 1993; **90**: 9150–4.
3 Liebowitz D, Wang D, Kieff E. Orientation and patching of the latent infection membrane protein encoded by Epstein-Barr virus. *J Virol* 1986; **58**: 233–7.
4 Hammarskjold ML, Simurda MC. Epstein-Barr virus latent membrane protein transactivates the human immunodeficiency virus type 1 long terminal repeat through induction of NF-κB activity. *J Virol* 1992; **66**: 6496–501.
5 Paine E, Scheinman RI, Baldwin AS Jr, Raab-Traub N. Expression of LMP1 in epithelial cells leads to the activation of a select subset of NF-κB/Rel family proteins. *J Virol* 1995; **69**: 4572–6.
6 Izumi KM, Kieff ED. The Epstein-Barr virus oncogene product latent membrane protein 1 engages the tumor necrosis factor receptor-associated death domain protein to mediate B lymphocyte growth transformation and activate NF-κB. *Proc Natl Acad Sci USA* 1997; **94**: 12592–7.
7 Kieser A, Kilger E, Gires O, Ueffing M, Kolch W, Hammerschmidt W. Epstein-Barr virus latent membrane protein-1 triggers AP-1 activity via the c-Jun N-terminal kinase cascade. *EMBO J* 1997; **16**: 6478–85.
8 Eliopoulos AG, Blake SM, Floettmann JE, Rowe M, Young LS. Epstein-Barr virus-encoded latent membrane protein 1 activates the JNK pathway through its extreme C terminus via a mechanism involving TRADD and TRAF2. *J Virol* 1999; **73**: 1023–35.
9 Eliopoulos AG, Gallagher NJ, Blake SM, Dawson CW, Young LS. Activation of the p38 mitogen-activated protein kinase pathway by Epstein-Barr virus-encoded latent membrane protein 1 coregulates interleukin-6 and interleukin-8 production. *J Biol Chem* 1999; **274**: 16085–96.
10 Roberts ML, Cooper NR. Activation of a ras-MAPK-dependent pathway by Epstein-Barr virus latent membrane protein 1 is essential for cellular transformation. *Virology* 1998; **240**: 93–9.
11 Gires O, Kohlhuber F, Kilger E *et al.* Latent membrane protein 1 of Epstein-Barr virus interacts with JAK3 and activates STAT proteins. *EMBO J* 1999; **18**: 3064–73.
12 Luo J, Manning BD, Cantley LC. Targeting the PI3K-Akt pathway in human cancer: rationale and promise. *Cancer Cell* 2003; **4**: 257–62.
13 Dawson CW, Tramountanis G, Eliopoulos AG, Young LS. Epstein-Barr virus latent membrane protein 1 (LMP1) activates the phosphatidylinositol 3-kinase/Akt pathway to promote cell survival and induce actin filament remodeling. *J Biol Chem* 2003; **278**: 3694–704.
14 Mainou BA, Everly DN Jr, Raab-Traub N. Epstein-Barr virus latent membrane protein 1 CTAR1 mediates rodent and human fibroblast transformation through activation of PI3K. *Oncogene* 2005; **24**: 6917–24.
15 Polakis P. Wnt signaling and cancer. *Genes Dev* 2000; **14**: 1837–51.
16 Korinek V, Barker N, Morin PJ *et al.* Constitutive transcriptional activation by a β-catenin-Tcf complex in APC-/- colon carcinoma. *Science* 1997; **275**: 1784–7.
17 Morin PJ. β-catenin signaling and cancer. *Bioessays* 1999; **21**: 1021–30.
18 Tomita M, Kikuchi A, Akiyama T, Tanaka Y, Mori N. Human T-cell leukemia virus type 1 tax dysregulates β-catenin signaling. *J Virol* 2006; **80**: 10497–505.
19 Miller G, Lipman M. Comparison of the yield of infectious virus from clones of human and simian lymphoblastoid lines transformed by Epstein-Barr virus. *J Exp Med* 1973; **138**: 1398–412.
20 Tomita M, Choe J, Tsukazaki T, Mori N. The Kaposi's sarcoma-associated herpesvirus K-bZIP protein represses transforming growth factor β signaling through interaction with CREB-binding protein. *Oncogene* 2004; **23**: 8272–81.

21 Ishiyama M, Tominaga H, Shiga M, Sasamoto K, Ohkura Y, Ueno K. A combined assay of cell viability and in vitro cytotoxicity with a highly water-soluble tetrazolium salt, neutral red and crystal violet. *Biol Pharm Bull* 1996; **19**: 1518–20.
22 Kishida M, Hino S, Michiue T *et al.* Synergistic activation of the Wnt signaling pathway by Dvl and casein kinase Iε. *J Biol Chem* 2001; **276**: 33147–55.
23 Kishida S, Yamamoto H, Ikeda S *et al.* Axin, a negative regulator of the wnt signaling pathway, directly interacts with adenomatous polyposis coli and regulates the stabilization of β-catenin. *J Biol Chem* 1998; **273**: 10823–6.
24 Shih IMYuJ, He TC, Vogelstein B, Kinzler KW. The β-catenin binding domain of adenomatous polyposis coli is sufficient for tumor suppression. *Cancer Res* 2000; **60**: 1671–6.
25 Huen DS, Henderson SA, Croom-Carter D, Rowe M. The Epstein-Barr virus latent membrane protein-1 (LMP1) mediates activation of NF-κB and cell surface phenotype via two effector regions in its carboxy-terminal cytoplasmic domain. *Oncogene* 1995; **10**: 549–60.
26 Floettmann JE, Rowe M. Epstein-Barr virus latent membrane protein-1 (LMP1) C-terminus activation region 2 (CTAR2) maps to the far C-terminus and requires oligomerisation for NF-κB activation. *Oncogene* 1997; **15**: 1851–8.
27 Sharma M, Chuang WW, Sun Z. Phosphatidylinositol 3-kinase/Akt stimulates androgen pathway through GSK3β inhibition and nuclear β-catenin accumulation. *J Biol Chem* 2002; **277**: 30935–41.
28 Dawson CW, Laverick L, Morris MA, Tramoutanis G, Young LS. Epstein-Barr virus-encoded LMP1 regulates epithelial cell motility and invasion via the ERK-MAPK pathway. *J Virol* 2008; **82**: 3654–64.
29 Arron JR, Vologodskaia M, Wong BR *et al.* A positive regulatory role for Cbl family proteins in tumor necrosis factor-related activation-induced cytokine (trance) and CD40L-mediated Akt activation. *J Biol Chem* 2001; **276**: 30011–17.
30 Suzuki H, Terauchi Y, Fujiwara M *et al.* Xid-like immunodeficiency in mice with disruption of the p85α subunit of phosphoinositide 3-kinase. *Science* 1999; **283**: 390–2.
31 Fujimuro M, Wu FY, ApRhys C *et al.* A novel viral mechanism for dysregulation of β-catenin in Kaposi's sarcoma-associated herpesvirus latency. *Nat Med* 2003; **9**: 300–6.
32 Shackelford J, Maier C, Pagano JS. Epstein-Barr virus activates β-catenin in type III latently infected B lymphocyte lines: association with deubiquitinating enzymes. *Proc Natl Acad Sci USA* 2003; **100**: 15572–6.
33 Morrison JA, Klingelhutz AJ, Raab-Traub N. Epstein-Barr virus latent membrane protein 2A activates β-catenin signaling in epithelial cells. *J Virol* 2003; **77**: 12276–84.

doi: 10.1111/j.1349-7006.2009.01121.x

Available online at
ScienceDirect
www.sciencedirect.com

Elsevier Masson France
EM|consulte
www.em-consulte.com

BIOMEDICINE & PHARMACOTHERAPY

ELSEVIER MASSON

Biomedicine & Pharmacotherapy 63 (2009) 703–706

Point of View

Natural killer activity of peripheral-blood mononuclear cells in breast cancer patients

Md. Zahidunnabi Dewan [a,b,1,2], Masahiro Takada [c,1], Hiroshi Terunuma [d,e], Xuewen Deng [d], Sunjida Ahmed [a], Naoki Yamamoto [a,b], Masakazu Toi [c,*]

[a] *Department of Molecular Virology, Graduate School, Tokyo Medical and Dental University, 1-5-45 Yushima, Bunkyo-ku, Tokyo 113-8519, Japan*
[b] *AIDS Research Center, National Institute of Infectious Disease, 1-23-1 Toyama, Shinjuku-ku, Tokyo 162-8640, Japan*
[c] *Department of Breast Surgery, Graduate School of Medicine, Kyoto University, 54 Kawaracho, Shogoin, Sakyo-ku, Kyoto 606-8507, Japan*
[d] *Biotherapy Institute of Japan, 2-4-8 Edagawa, Koutou-ku, Tokyo 135-0051, Japan*
[e] *Tokyo Clinic Marunouchi Oazo mc, Shin-Marunouchi Center Building, 1-6-2 Marunouchi, Chiyoda-ku, Tokyo 100-0005, Japan*

Received 23 January 2009; accepted 11 February 2009
Available online 25 February 2009

Abstract

Natural killer (NK) activity of immune cells plays a central role in host defense against cancer and virus-infected cells. Natural cytotoxic activity of peripheral-blood mononuclear cells was assessed by a Calcein-AM release assay in 89 subjects. In the present study, we here demonstrated that NK activities of peripheral-blood mononuclear cells (PBMCs) from breast cancer patients were significantly lower as compared with that of healthy individuals. There were significant differences in the NK activities of PBMCs from HER2-negative breast cancer patients as compared with HER2-positive patients. Our results suggest that NK activity of PBMCs is lower in breast cancer indicating a role for immunological natural host defense mechanisms against cancer.

Keywords: NK activity; Breast cancer; NK cell; PBMCs

1. Introduction

Cancer metastasis is the result of several sequential steps and represents a highly organized, non-random and organ-selective process [1]. Immune cells and a wide number of molecules have been implicated to be responsible for the primary growth and metastatic property of cancer cells [2–5]. Breast cancer is characterized by a distinct pattern of metastasis involving regional lymph nodes, bone marrow, lung and liver.

Natural killer (NK) cells are large granular lymphocytes that mediate innate immunity against pathogens and tumors [6]. NK cells were originally discovered because of their ability to kill tumor and virally infected cells without exposure to the target cell antigens. One study showed that individuals with low natural cytotoxic activity of peripheral-blood lymphocytes are at a significantly higher risk of cancer, compared with those of median or high activity [7]. It has been reported that NK cells isolated from HIV-infected individuals are impaired in their ability to kill the virus-infected autologous cells [8–11]. NK cells are capable of mediating antibody-dependent cell cytotoxicity (ADCC) against antibody-coated targets via their expression of a low-affinity receptor for IgG (FcγRIII or CD16). The humanized version of the anti-HER2/neu mAb (Trastuzumab) exhibits improved binding affinity to the extracellular R domain of Her2/neu and mediates potent growth inhibitory activity against Her2/neu-overexpresssing cell lines and xenografts [12]. In murine models, experimental data have

* Corresponding author at: Department of Breast Surgery, Graduate School of Medicine, Kyoto University, 54 Kawaracho, Shogoin, Sakyo-ku, Kyoto 606-8507, Japan.
E-mail address: toi@kuhp.kyoto-u.ac.jp (M. Toi).
[1] M.Z. Dewan and M. Takada equally contribute to this report.
[2] Present address: Department of Pathology, New York University School of Medicine, 550 First Avenue, New York, NY 10016, USA.

0753-3322/$ - see front matter © 2009 Elsevier Masson SAS. All rights reserved.
doi:10.1016/j.biopha.2009.02.003

shown that ADCC is an important anti-tumor mechanism utilized in vivo against Her2/neu+ tumor cells [13,14]. ADCC conducted by NK cells in vitro is enhanced by IL-2 activation and is critically dependent on interactions between FcγRIII on NK cells and Trastuzumab-coated tumor targets [15]. Clynes et al. have shown that the anti-tumor effects of Trastuzumab in a murine model of breast cancer require the expression of functional Fc receptors by immune effectors [16]. Blockade of FCγRIII with anti-CD16 mAb inhibited ADCC by approximately 80% compared to NK cells incubated with control IgG [15]. Recently, our studies reported that involvement of NK cells is critical for tumor growth and metastasis of cancer and virus-infected cells in murine model [17,18] and autologous activated NK cells could be useful for cancer and viral immunotherapy [19]. However, role of natural killer activities in the course of cancer progression in human remains one of the major issues in tumor immunology and immunotherapy.

In the present study, we investigated the natural killer activities of breast cancer patients. We found that natural killer activities of peripheral-blood mononuclear cells (PBMCs) from breast cancer patients were substantially lower than from healthy individuals. HER2-negative breast cancer patients had lower natural killer activity as compared with HER2-positive patients. Thus, our results suggest that natural killer activity of immune cells might play a critical role to progression of cancer in patients.

2. Materials and methods

2.1. Collection of human specimens and isolation of PBMCs

The Ethical Review Committee of the Institute approved the experimental protocol. Blood was collected after obtaining informed consent from breast cancer patients and healthy volunteers. PBMCs were isolated from the blood by Ficoll-Hypaque gradient centrifugation (Amersham Biosciences, Uppsala, Sweden) and washed twice with RPMI1640 and counted the number of cells by trypan blue.

2.2. Culture of cell line

Erythroleukemia cell line K562 was cultured in RPMI1640 medium supplemented with 10% heat-inactivated fetal bovine serum (JRH Biosciences, Lenexa, KS), 100 U/ml penicillin, and 10 μg/ml streptomycin.

2.3. Cytotoxic activity

Freshly isolated PBMCs and activated NK cells were tested for cytotoxic activity at various effector-to-target (E/T) ratios in a Calcein-AM release assay using TERASCAN VP (Minerva Tech., Tokyo, Japan). We labeled the target cells K562 with immunofluorescent-dye Calcein-AM solution (Do Jindo Lab., Kumamoto, Japan) and incubated for 30 min and followed by washing the cells with PBS(−) and checked the fluorescence intensity of cells. Target cells and effector cells were suspended with RPMI1640 and 10% fetal bovine serum at various E/T ratios and added into 96-well plate and followed by incubation for 2 h and again checked the fluorescence intensity.

2.4. Statistical analysis

The statistical analysis was performed using StatView for Windows, Version 5.0.

3. Results and discussion

Totally 89 individuals were enrolled in this study and agreed to give peripheral-blood samples. Among them 71 were breast cancer patients (61 primary and 10 metastatic patients) and 18 healthy volunteers. Baseline characteristics for primary cancer patients who entered the study are shown in Table 1. Average age of healthy donors is 30 (20–70) years, used in this study as control, average age of primary breast cancer patients is 55 (31–84) years and average age of metastatic cancer patients is 59 (36–69) years.

Table 1
Clinico-pathological data of the primary breast cancer patients.

	$n = 61$
Age	
Median (min–max)	55 (31–84)
Menopause	
Pre	21 (34.4%)
Post	40 (65.6%)
Histological type	
Ductal carcinoma in situ	7 (11.5%)
Invasive ductal carcinoma	50 (82.0%)
Others	3 (4.9%)
Unknown	1 (1.6%)
Tumor size	
T1	17 (27.9%)
T2	37 (60.7%)
T3	6 (9.8%)
T4	1 (1.6%)
Lymph node	
N0	41 (67.3%)
N1	18 (29.5%)
N2	1 (1.6%)
Unknown	1 (1.6%)
Estrogen receptor	
Positive	37 (60.6%)
Negative	14 (23.0%)
Unknown	10 (16.4%)
Progesterone receptor	
Positive	27 (44.3%)
Negative	24 (39.3%)
Unknown	10 (16.4%)
HER2 (IHC[a])	
0	14 (23.0%)
1+	22 (36.1%)
2+	6(9.8%)
3+	8 (13.1%)
Unknown	11 (18.0%)

[a] Immunohistochemical (HercepTest™).

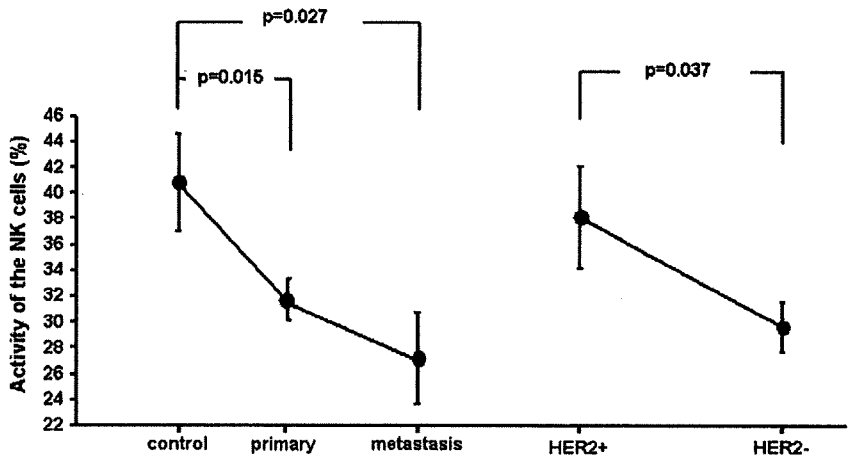

Fig. 1. NK activity in cancer patients. Spontaneous cytotoxic activity of freshly isolated PBMCs from breast cancer patients was done against K562 cells at different E/T ratios. Averages were calculated on healthy donors versus various cancer patients with statistical analysis. Natural killer activity of breast cancer patients with primary and metastatic tumor was compared with healthy donors and natural killer activity of breast cancer patients with HER2-positive (IHC 2+ and 3+) and -negative (IHC 0 and 1+). The number of healthy donors 18 and number of patients such as primary 61, metastasis 10, HER2-positive 14 and -negative 36 were enrolled in this study.

In patients with cancer and viral infection, NK-cell function has been shown to be impaired [20,21]. To check the natural killer activity, we examined the natural cytotoxic activity of freshly isolated PBMCs from patients with breast cancer and healthy individuals against susceptible K562 erythroleukemia cell line. Natural killer activity of PBMCs was significantly lower in patients with breast cancer than that of healthy individuals (Fig. 1 and Table 2). Furthermore, the ability to kill K562 target cells was clearly reduced in PBMCs from HER2-negative 36 cancer patients than 14 patients with HER2-positive tumors (Fig. 1). No statistical association was found between the natural killer activities and primary and metastatic tumor, tumor sizes, age groups and hormone receptors (data not shown). Total number of T cells and lymphocytes were substantially lower in breast cancer patients as compared with healthy donors (Table 2). There were no statistical differences among the two groups of study subjects in the median number of NK cells and its subsets and WBC (Table 2). These results suggest that natural killer activities are important for breast cancer development and disease progression.

Table 2
Immunological status of the patients and healthy donors.

	Patients	Healthy donors	*p*-value (*t*-test)
Natural killer activity (%)	31.1	40.8	0.007
Number of the NK cells (/microL)	137.5	167.1	N.S.
Number of the CD16+/CD56 − cells (/microL)	34.1	35.6	N.S.
Number of the CD16+/CD56 + cells (/microL)	134.9	155.2	N.S.
Number of the CD4+/CD25 + cells (/microL)	74.5	32.5	N.S.
Number of the T cells (/microL)	724.7	959.5	0.004
Number of the lymphocyte (/microL)	1064.9	1438.5	0.002
Number of the WBC (/microL)	4644.2	5176.9	N.S.

In summary, our results suggest that NK activity of immune cells may play a critical role in tumor growth and metastasis, and that autologous activated NK cells could be a promising immunotherapeutic strategy against cancer either alone or in combination with humanized anti-tumor antibodies as a logical approach to the immunotherapy of cancer.

Conflict of interest

The authors have declared that no conflict of interest exists.

Acknowledgements

This work was supported by grants from the Ministry of Education, Science and Culture; the Ministry of Health, Labor and Welfare; and Human Health Science of Japan.

References

[1] Nicolson GL. Paracrine and autocrine growth mechanisms in tumor metastasis to specific sites with particular emphasis on brain and lung metastasis. Cancer Metastasis Rev 1993;12:325–43.
[2] Kim H, Muller WJ. The role of the epidermal growth factor receptor family in mammary tumorigenesis and metastasis. Exp Cell Res 1999; 253:78–87.
[3] Hyder SM, Chiappetta C, Stancel GM. Pharmacological and endogenous progestins induce vascular endothelial growth factor expression in human breast cancer cells. Int J Cancer 2001;92:469–73.
[4] McEarchern JA, Kobie JJ, Mack V, Wu RS, Meade-Tollin L, Arteaga CL, et al. Invasion and metastasis of a mammary tumor involves TGF-beta signaling. Int J Cancer 2001;91:76–82.
[5] Muller A, Homey B, Soto H, Ge N, Catron D, Buchanan ME, et al. Involvement of chemokine receptors in breast cancer metastasis. Nature 2001;410:50–6.
[6] Trinchieri G. Biology of natural killer cells. Adv Immunol 1989;47:187–376.
[7] Imai K, Matsuyama S, Miyake S, Suga K, Nakachi K. Natural cytotoxic activity of peripheral-blood lymphocytes and cancer incidence: an 11-year follow-up study of a general population. Lancet 2000;356:1795–9.

[8] Ullum H, Gotzsche PC, Victor J, Dickmeiss E, Skinhøj P, Pedersen BK. Defective natural immunity: an early manifestation of human immunodeficiency virus infection. J Exp Med 1995;182:789–99.
[9] Ahmad R, Menezes J. Defective killing activity against gp120/41-expressing human erythroleukaemic K562 cell line by monocytes and natural killer cells from HIV-infected individuals. AIDS 1996;10:143–9.
[10] Scott-Algara D, Paul P. NK cells and HIV infection: lessons from other viruses. Curr Mol Med 2002;2:757–68.
[11] Bonaparte MI, Barker E. Inability of natural killer cells to destroy autologous HIV-infected T lymphocytes. AIDS 2003;17:487–94.
[12] Carter P, Presta L, Gorman CM, Ridgway JB, Henner D, Wong WL, et al. Humanization of an anti-p185HER2 antibody for human cancer therapy. Proc Natl Acad Sci U S A 1992;89:4285–9.
[13] Tokuda Y, Ohnishi Y, Shimamura K, Iwasawa M, Yoshimura M, Ueyama Y, et al. In vitro and in vivo anti-tumour effects of a humanised monoclonal antibody against c-erbB-2 product. Br J Cancer 1996;73:1362–5.
[14] Sliwkowski MX, Lofgren JA, Lewis GD, Hotaling TE, Fendly BM, Fox JA. Nonclinical studies addressing the mechanism of action of trastuzumab (Herceptin). Semin Oncol 1999;26:60–70.
[15] Carson WE, Parihar R, Lindemann MJ, Personeni N, Dierksheide J, Meropol NJ, et al. Interleukin-2 enhances the natural killer cell response to Herceptin-coated Her2/neu-positive breast cancer cells. Eur J Immunol 2001;31:3016–25.
[16] Clynes RA, Towers TL, Presta LG, Ravetch JV. Inhibitory Fc receptors modulate in vivo cytoxicity against tumor targets. Nat Med 2000;6:443–6.
[17] Dewan MZ, Terunuma H, Takada M, Tanaka Y, Abe H, Sata T, et al. Role of natural killer cells in hormone-independent rapid tumor formation and spontaneous metastasis of breast cancer cells in vivo. Breast Cancer Res Treat 2007;104:267–75.
[18] Dewan MZ, Terunuma H, Toi M, Tanaka Y, Katano H, Deng X, et al. Potential role of natural killer cells in controlling growth and infiltration of AIDS-associated primary effusion lymphoma cells. Cancer Sci 2006;97:1381–7.
[19] Terunuma H, Deng X, Dewan MZ, Fujimoto S, Yamamoto N. Potential role of NK cells in the induction of immune responses: implications for NK cell-based immunotherapy for cancers and viral infections. Int Rev Immunol 2008;27:93–110.
[20] Whiteside TL, Herberman RB. Role of human natural killer cells in health and disease. Clin Diagn Lab Immunol 1994;1:125–33.
[21] Whiteside TL, Vujanovic NL, Herberman RB. Natural killer cells and tumor therapy. Curr Top Microbiol Immunol 1998;230:221–44.

Int. J. Cancer: **124,** 622–629 (2009)

An HIV protease inhibitor, ritonavir targets the nuclear factor-kappaB and inhibits the tumor growth and infiltration of EBV-positive lymphoblastoid B cells

Md. Zahidunnabi Dewan[1,2], Mariko Tomita[3], Harutaka Katano[4], Norio Yamamoto[1], Sunjida Ahmed[1], Michiko Yamamoto[5], Tetsutaro Sata[4], Naoki Mori[3]* and Naoki Yamamoto[1,2]*

[1]*Department of Molecular Virology, Graduate School, Tokyo Medical and Dental University, 1-5-45 Yushima, Bunkyo-ku, Tokyo 113-8519, Japan*
[2]*AIDS Research Center, National Institute of Infectious Diseases, 1-23-1 Toyama, Shinjuku-ku, Tokyo 162-8640, Japan*
[3]*Division of Molecular Virology and Oncology, Graduate School of Medicine, University of the Ryukyus, 207 Uehara, Nishihara, Okinawa 903-0215, Japan*
[4]*Department of Pathology, National Institute of Infectious Diseases, 1-23-1 Toyama, Shinjyuku-ku, Tokyo 162-8640, Japan*
[5]*Division of Safety Information on Drug, National Institute of Health Sciences, Food and Chemicals, Setagaya-ku, Tokyo 158-8501, Japan*

Epstein-Barr Virus (EBV)-associated immunoblastic lymphoma occurs in immunocompromised patients such as those with AIDS or transplant recipients after primary EBV infection or reactivation of a preexisting latent EBV infection. In the present study, we evaluated the effect of ritonavir, an HIV protease inhibitor, on EBV-positive lymphoblastoid B cells *in vitro* and in mice model. We found that it induced cell-cycle arrest at G_1-phase and apoptosis through down-regulation of cell-cycle gene cyclin D2 and anti-apoptotic gene survivin. Furthermore, ritonavir suppressed transcriptional activation of NF-κB in these cells. Ritonavir efficiently prevented growth and infiltration of lymphoma cells in various organs of NOD/SCID/γc^{null} mice at the same dose used for treatment of patients with AIDS. Our results indicate that ritonavir targets NF-κB activated in tumor cells and shows anti-tumor effects. These data also suggest that this compound may have promise for treatment or prevention of EBV-associated lymphoproliferative diseases that occur in immunocompromised patients.

Key words: ritonavir; LCLs; NF-κB; NOG mice

Epstein-Barr virus (EBV) is a ubiquitous human γ herpes virus that establishes a latent infection more than 90% of adults worldwide.[1] Immunocompromised individuals such as those with AIDS or transplant recipients are at increased risk for developing aggressive EBV-associated lymphoproliferative diseases. EBV is associated with malignant diseases, including Burkitt's lymphoma,[1,2] nasopharyngeal carcinoma[3,4] and immunoblastic B cell lymphoma of immunosuppressed individuals. Infection of primary B cells with EBV results in transformation with growth of the cells in tight clumps and immortalization of the cells. These immortalized B cells have an immunoblastic morphology and express each of the EBV-encoded small RNAs (EBERs), EBV nuclear antigen (EBNAs) and latent membrane proteins (LMPs).[2,5] EBERs have oncogenic potential through inhibition of PKR.[6] EBNA-2 is a transactivator that up-regulates expression of cellular genes and LMPs. LMP-1 may mediate proliferative and survival effects not only in EBV-transformed B lymphocytes but also in these malignancies that occur long after primary infection. Many immunocompromised patients with EBV-associated immunoblastic lymphoma have tumors at extranodal sites such as the brain, lung, or gastrointestinal tract. The prognosis of EBV-associated lymphomas is very poor for patients with irreversible immunosuppression and treatment options are limited.

Despite the diversity in clinical manifestations of hematopoietic malignancies, strong and constitutive nuclear factor-kappaB (NF-κB) activation was reported to be a unique and common characteristic of malignant cells.[7,8] In resting cells, NF-κB is sequestered as an inactive precursor by association with inhibitory IκBs in the cytoplasm. On stimulation, IκBs are rapidly phosphorylated, ubiquitinated and degraded by a proteasome-dependent pathway allowing active NF-κB to translocate into the nucleus where it can activate the expression of a number of genes.[9] LMP-1 is an oncoprotein that constitutively activates NF-κB to induce B cell proliferation.[7] Lymphoblastoid cell lines (LCLs) express high level of the antiapoptotic proteins BCL-2, BCL-xL, c-IAP1, Bfl-1 and c-FLIP the targets of NF-κB.[10,11] NF-κB activation has been connected with multiple processes of oncogenesis including control of apoptosis, cell-cycle, differentiation and cell migration,[9] and therefore, inhibition of NF-κB was suggested to be a useful strategy for cancer therapy.[12–20] It has been also reported that inhibition of NF-κB in EBV-associated lymphomas results in induction of apoptosis.[21] Therefore, targeting the NF-κB pathway and inhibition of NF-κB activity is a logical strategy for treating EBV-associated lymphomas.

Ritonavir, a human immunodeficiency virus type 1(HIV-1) protease inhibitor, has been successfully used in clinical treatments of HIV infection, with patients exhibiting a marked decrease in HIV viral load and a subsequent increase in $CD4^+$ T-cell counts.[22–25] Evidence of other effects by ritonavir on cellular proteases, such as the cysteine proteases cathepsin D and E, was presented in the drug's original description, albeit at concentrations >500-fold above the concentration required for inhibition of HIV protease.[26] Protease inhibitors have also been shown to directly affect cell metabolism, interfere with host or fungal proteases and block T-cell activation and dendritic-cell function.[27,28] Ritonavir has been shown to inhibit the chymotrypsin-like activity of the 20S proteasome, and it activates the chymotrypsin-like activity of the 26S proteasome conversely.[27,29,30] Ritonavir also has been reported to inhibit the transactivation of NF-κB induced by activators such as TNFα, HIV-1 Tat protein and the human herpesvirus 8 protein ORF74.[31] It is possible that inhibition of NF-κB activation by ritonavir is linked to additional pathways other than inhibition of proteasome.[31] Protease inhibitors also have been shown to have direct antiangiogenic and antitumor activity.[31,32] Recently, we reported that ritonavir inhibits growth and infiltration of ATL cells through targeting NF-κB.[20]

Grant sponsors: Ministry of Education, Science and Culture, The Ministry of Health, Labor and Welfare, Human Health Science of Japan.

Md. Zahidunnabi Dewan's current address is: Department of Pathology, New York University School of Medicine, 550 First Avenue, New York, NY 10016, USA.

Md. Zahidunnabi Dewan and Mariko Tomita contributed equally to this work.

***Correspondence to:** AIDS Research Center, National Institute of Infectious Diseases, 1-23-1 Toyama, Shinjuku-ku, Tokyo 162-8640, Japan. Fax: 8135-285-1165. E-mail: nyama@nih.go.jp (or) Division of Molecular Virology and Oncology, Graduate School of Medicine, University of the Ryukyus, 207 Uehara, Nishihara, Okinawa 903-0215, Japan. Fax: 81-98-895-1410. E-mail: n-mori@med.u-ryukyu.ac.jp.

Received 14 July 2008; Accepted after revision 2 September 2008
DOI 10.1002/ijc.23993
Published online 15 September 2008 in Wiley InterScience (www.interscience.wiley.com).

Publication of the International Union Against Cancer

In the present, we demonstrate that inhibition of NF-κB activity by ritonavir results in marked increase of apoptosis and induce cell-cycle arrest in EBV-positive lymphoblastoid B cells. We found that ritonavir also suppresses the expression of genes involved in antiapoptosis and cell-cycle progression. In addition, we established preclinical models using newly developed NOD/SCID/γc^{null} (NOG) mouse,[16] a unique type of animal, lacking T-, B- and NK-cells to evaluate the efficacy of antitumor and anti-NF-κB therapies. In the murine model, ritonavir at the clinically relevant dose potently inhibited the growth and infiltration of EBV-transformed LCL cells.

Material and methods

Mice and cells

NOG mice were obtained from the Central Institute for Experimental Animals (Kawasaki, Japan). All mice were maintained under specific-pathogen-free conditions in the Animal Center of Tokyo Medical and Dental University (Tokyo, Japan). The Ethical Review Committee of the Institute approved the experimental protocol.

EBV-positive immortalized lymphoblatoid B-cell lines (LCL-Ya, LCL-Ao, LCL-Ka and LCL-Ku) were cultured in RPMI 1640 medium supplemented with 10% heat-inactivated fetal bovine serum (JRH Biosciences, Lenexa, KS), 100 U/ml penicillin, and 10 μg/ml streptomycin. Peripheral blood mononuclear cells (PBMCs) from 3 healthy volunteers were analyzed. Mononuclear cells were isolated by Ficoll-Paque density gradient centrifugation (GE Healthcare Biosciences, Uppsala, Sweden) and washed with PBS.

Cell viability assay

The effect of ritonavir on cell viability of LCLs and PBMCs from healthy donors was examined by the reagent, water-soluble tetrazolium (WST)-8 (Wako Chemicals, Osaka, Japan). Briefly, 2×10^5 cells were incubated in a 96-well microculture plate in the absence or presence of various concentrations of ritonavir. After 72 hr of culture, WST-8 (5 μl) was added for the last 4 hr of incubation and absorbance at 450 nm was measured using an automated microplate reader. Measurement of mitochondrial dehydrogenase cleavage of WST-8 to formazan dye provides an indication of the level of cell viability.

Cell-cycle analysis

Cells were plated at a density of 3×10^5/ml in 60-mm tissue culture dishes. Twelve hours after plating, cells were exposed to 40 μM ritonavir for 24 h. Cell-cycle analysis was performed with the CycleTEST PLUS DNA reagent kit (Becton Dickinson, San Jose, CA). Briefly, cells were washed with a buffer solution containing sodium citrate, sucrose and dimethyl sulfoxide, suspended in a solution containing RNase A, and stained with 125 μg/ml propidium iodide (PI) for 10 min. Cell suspensions were analyzed on EPICS XL flow cytometer (Beckman Coulter, Fullerton, CA) using EXPO32 software. The cell population at each cell-cycle phase was determined with MultiCycle software (Beckman Coulter).

Assay for apoptosis

Cells were plated at a density of 3×10^5/ml in 60-mm tissue culture dishes. Twelve hours after plating, cells were exposed to ritonavir for 72 hr. Apoptosis was quantified by double staining with Annexin-V-Fluos (Roche Diagnostics, Mannheim, Germany) and PI (Backman Coulter) according to the instructions supplied by the manufacturer. Cells were analyzed on EPICS XL flow cytometer (Beckman Coulter) using EXPO32 software.

Western blot analysis

Treated cells were solubilized at 4°C in lysis buffer containing 62.5 mM Tris-HCl (pH 6.8), 2% SDS, 10% glycerol, 6% 2-mercaptoethanol and 0.01% bromophenol blue. Samples were subjected to electrophoresis on SDS-polyacrylamide gels followed by transfer to a polyvinylidine difluoride membrane and probing with the following specific antibodies: polyclonal antibodies against survivin, cyclin D2 (Santa Cruz Biotechnology, Santa Cruz, CA), Bcl-X_L (BD Transduction Laboratories, San Jose, CA) and monoclonal antibodies against Bcl-2, p53, actin (NeoMarkers, Fremont, CA), PARP (BD Transduction Laboratories) and LMP-1 (DAKO, Kyoto, Japan). The protein bands recognized by the antibodies were visualized using the enhanced chemiluminescence system (Amersham, Piscataway, NJ).

Electrophoresis mobility shift assay (EMSA)

Cells were placed in culture at 1×10^6 cells/ml and examined for inhibition of NF-κB 24 hr after exposure to ritonavir. Nuclear proteins were extracted, and NF-κB binding activities to κB element were examined by EMSA as described previously.[8] In brief, 5 μg of nuclear extracts were preincubated in a binding buffer containing 1 μg of poly (dI:dC) (Amersham Biosciences), followed by addition of ^{32}P-labeled oligonucleotide probe containing NF-κB element (5×10^4 c.p.m.). These mixtures were incubated for 15 min at room temperature. The DNA-protein complexes were separated on a 4% polyacrylamide gel and visualized by autoradiography. To examine the specificity of the NF-κB element probe, unlabeled competitor oligonucleotides were preincubated with nuclear extracts for 15 min before incubation with probes. The probe or competitors used were prepared by annealing the sense and antisense synthetic oligonucleotides as follows: a typical NF-κB element from the *IL-2Rα* gene, 5′-gatcCGGCAGGGGAATCTCCCTCTC-3′; and AP-1 element of the *IL-8* gene, 5′-gactGTGATGACTCAGGTT-3′. Underlined sequences represent the NF-κB or AP-1 binding site. To identify NF-κB protein in the DNA protein complex revealed by EMSA, we used antibodies specific for various NF-κB proteins, including p50, p65, c-Rel, RelB and p52 (Santa Cruz Biotechnology), to elicit a supershift DNA protein complex formation. These antibodies were incubated with the nuclear extracts for 45 min at room temperature before incubation with radiolabeled probes.

Inoculation of EBV-positive immortalized LCLs and collection of samples

LCL Cells [LCL-Ya, LCL-Ao, LCL-Ka and LCL-Ku] were washed twice with serum-free RPMI-1640 medium and resuspended in same medium. Mice were anaesthetized with ether and cells were inoculated subcutaneously (sc) in the postauricular region of NOG mice at a dose of 1×10^7 cells per mouse. All mice were sacrificed 3 weeks after inoculation with lymphoma cells. We measured tumor size 3 weeks after inoculation. Tissues and various organs of mice were collected and fixed with Streck Tissue Fixative, then processed to paraffin wax-embedded sections for staining with hematoxylin and eosin (HE) and immunostaining.

PCR primer and conditions

Detection of the BamHI W repeat region of the EBV genome was performed using 100 ng of genomic DNA extracted from LCLs as follows. LCLs were lysed with genomic DNA extraction buffer (100 mM Tris-HCl pH8.0, 5 mM EDTA, 0.2% SDS, 200 mM NaCl and 200 μg/mL proteinase K) and the lysate was incubated at 50°C for 3 hr. After phenol-chloroform extraction, genomic DNA was purified by ethanol precipitation procedure. A 121-bp fragment of the EBV W repeat region was amplified by the forward primer 5′-CGCATAATGGCGGACCTAG-3′ and reverse primer 5′-CAAACAAGCCCACTCCCC-3′ in a 25 μl reaction mixture comprising 1 × AmpliTaq Gold buffer, 3.5 mM MgCl2, 200 μM dNTP, 300 nM primers, 200 nM probe and 0.025 U/μl AmpliTaq Gold. The PCR cycle conditions were as follows: a DNA denaturation and polymerase activation step of 10 min at 95°C and then 40 cycles of amplification (95°C for 15 sec, 60°C for 1 min). PCR products were separated by electrophoresis on agarose gels, stained with ethidium bromide and visualized by UV-light.

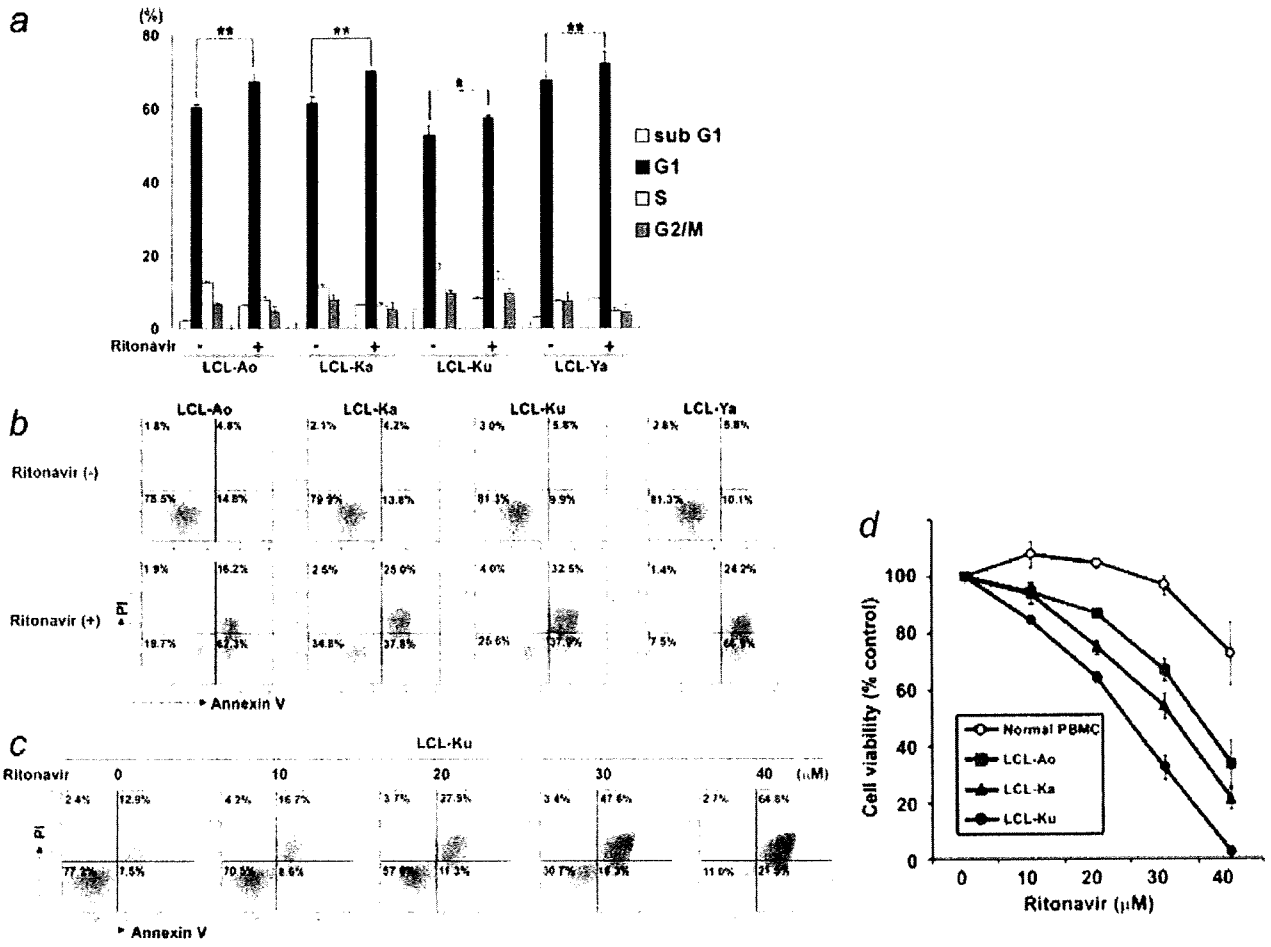

FIGURE 1 – Effect of ritonavir on cell cycle arrest and induction of apoptosis of EBV-positive lymphoblastoid B cells. (*a*) Effect of ritonavir on cell cycle progression of EBV-positive lymphoblastoid B cells. Cells were cultured for 24 hr with (+) or without (−) ritonavir (40 μM). DNA content was analyzed by flow cytometry with PI staining. Sub G_1, S and G_2/M indicate the stages of the cell cycle. Data are expressed as the mean percentages of the cells from three independent experements. Significance of differences between % G_1 of ritonavir treated (+) and untreated (−) cells calculated by Student's *t*-test is shown as *P*-value with astalisk(s). $*p < 0.05$ and $**p < 0.01$. (*b*) Effect of ritonavir on induction of apoptosis of EBV-immortalized B-cell lines. Cells were cultured for 72 hr with (+) or without (−) ritonavir (40 μM). (*c*) Ritonavir induces apoptosis of EBV-immortalized B-cell lines in a dose-dependent manner. LCL-Ku cells were cultured for 72 hr with increasing concentration of ritonavir (0, 10, 20, 30, 40 μM). Cells were harvested and stained with Annexin-V and PI. Apoptosis was analyzed by flow cytometry. Bottom left quadrants, viable cells; bottom right quadrants, early apoptotic cells. Top right quadrants, nonviable, late apoptotic/necrotic cells. (*d*) Effect of ritonavir on cell viability of LCLs and PBMCs from normal healthy controls. LCLs and PBMCs were incubated in the presence of various concentrations of ritonavir for 72 hr and viability of the cultured cells was measured by WST-8 assay. Relative viability of the cultured cells is presented as the mean determined on LCLs and PBMCs from triplicate cultures. A relative viability of 100% was designated as total number of cells that grew in 72-hr cultures in the absence of ritonavir.

Treatment of tumor-bearing mice with ritonavir

Ritonavir was obtained from Abbott Labs, North Chicago, IL. LCL-Ku cells (1×10^7) were inoculated s.c. in the post-auricular region of NOG mice. The drug was administered s.c. into the tumor cells inoculated site of mice at doses of 30 mg/kg/day, beginning on day 0 for 3 weeks. The control mice received RPMI-1640 (200 μl) simultaneously. In other experiments, ritonavir or RPMI-1640 was also administered intraperitoneally into mice as the same doses stated above, beginning on day 4 for 18 days.

In situ *hybridization*

EBERs were detected by *in situ* hybridization using fluorescein isothiocyanate (FITC)-conjugated EBER PNA (peptide nucleic acid)-probe (DAKO). Briefly, formalin-fixed, paraffin-embedded tissue sections of tumor and various organs were deparaffinized and hydrated in xylenes and graded alcohol series, then rinsed for 5 min in PBS. Deparaffinized samples were incubated with 10 ng/μl of proteinase K for 20 min at 37°C followed by washing, and then incubated with 0.3% methanol for 30 min at room temperature. After washing in PBS, the sections were hybridized with FITC-conjugated EBER-PNA probe in the hybridization solution for 90 min at 56°C. The slides were washed twice in 0.2 × SSC for 20 min at 56°C, and incubated with anti-FITC monoclonal antibody (DAKO) for 45 min at 37°C. Followed by washing, the slides were incubated with horse-radish peroxidase-conjugated polymer reagent (Envision, DAKO) for 30 min at room temperature. Positive staining was visualized after incubation of these samples with a mixture of 0.05% 3,3′-diaminobenzidine tetrahydrochloride in 50 mM Tris-HCl buffer pH7.6 and 0.01% hydrogen peroxide for 5 min. The samples were counterstained with hematoxlin for 2 min, hydrated completely, cleaned in xylene and then mounted. The samples were visualized and photographed under light microscopy (BX41 and DP70; Olympus, Tokyo, Japan).

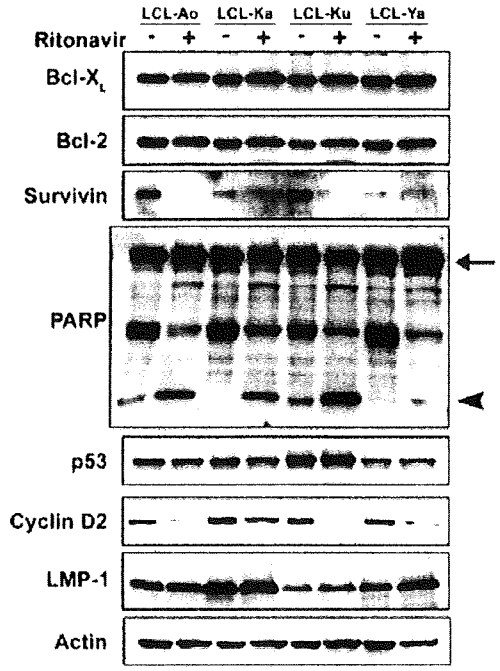

FIGURE 2 – Ritonavir inhibits expression of apoptosis- and cell cycle-associated proteins. EBV-immortalized B-cell lines were cultured with (+) or without (−) ritonavir (40 μM) for 24 hr. Cells were harvested and subjected to Western blot analysis. The polyvinylidene fluoride membrane was sequentially probed with indicated antibodies. Arrow indicates full-length PARP (116 kDa) and arrow head indicates cleaved form of PARP (25 kDa). Essentially the same results were obtained in 3 experiments and representative data are shown.

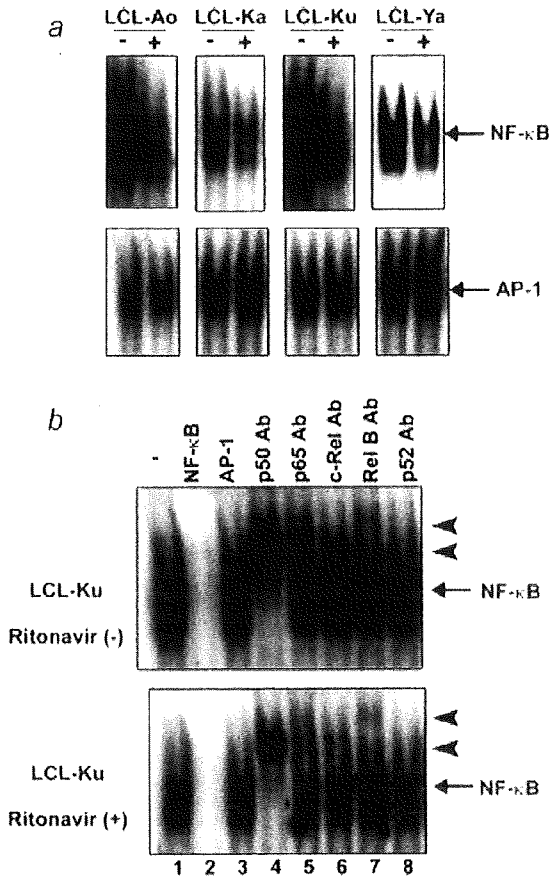

FIGURE 3 – Ritonavir inhibits constitutive NF-κB activation. (*a*) EBV-immortalized B-cell lines were cultured with (+) or without (−) ritonavir (40 μM) for 24 hr and assessed for NF-κB and AP-1-DNA binding activity. (*b*) Cold competition using 100-fold excess of unlabeled NF-κB oligonucleotide, or AP-1 oligonucleotide (lanes 2–3) demonstrated the specificity of the protein/DNA binding complexes. Specificity of NF-κB binding was also determined by using antibodies to the NF-κB components p50, p65, c-Rel, RelB and p52, resulting in supershift (lanes 4–8). Arrows indicate specific complexes of NF-κB with wild type NF-κB oligonucleotide. Arrow heads indicate supershift. Essentially the same results were obtained in 3 experiments and representative data are shown.

Results

Ritonavir induces cell-cycle arrest and apoptosis of LCLs

Ritonavir was examined for its effect on cell-cycle distribution of EBV-immortalized LCLs (Fig. 1*a*). Ritonavir effectively inhibited cell-cycle progression, as evidenced by increased proportion of the cells in G_1 phase of LCL-Ao, LCL-Ka, LCL-Ku and LCL-Ya (LCL-Ao: from 60.1% to 67.1%; LCL-Ka: from 61.2% to 69.9%; LCL-Ku: from 52.6% to 57.3%; and LCL-Ya: from 67.4% to 72.1%). These results indicated that ritonavir induced cell-cycle arrest at G_1-phase. The weak accumulation of cells in G_1 phase by ritonavir suggests that it might rather be an apoptosis inducer than a cell growth inhibitor.

Furthermore, we evaluated the effect of ritonavir on the cell viability of LCLs and PBMCs from healthy individuals (Fig. 1*d*). Ritonavir effectively reduced the survival of LCLs (LCL-Ao, LCL-Ka and LCL-Ku) as measured by WST-8 on the third day of culture in a dose-dependent manner. In contrast, ritonavir hardly affected the survival of PBMCs from healthy volunteers.

The effect of ritonavir on apoptosis was examined by the Annexin-V and PI method. Annexin-V binds to the cells that express phosphatidylserine on the outer layer of the cell membrane, a characteristic feature of cells entering apoptosis. Early apoptotic cells were stained with Annexin V but not with PI. Late apoptotic and necrotic cells were stained with both fluorescent. Ritonavir induced increased proportion of cells positive for Annexin-V and negative for PI in all cell lines (LCL-Ao: from 14.8% to 62.3%; LCL-Ka: from 13.8% to 37.8%; LCL-Ku: from 9.9% to 37.9% and LCL-Ya: from 10.1% to 66.9%) (Fig. 1*b*). Ritonavir also induced dose-dependent increasing of Annexin-V positive and PI negative cells in LCL-Ku cells (Fig. 1*c*), indicating increasing apoptosis of ritonavir-treated cells.

Ritonavir down-regulates the expression of the cell-cycle- and apoptosis-associated genes

The antiproliferative and proapoptotic effects of ritonavir were explored by examining the levels of intracellular regulators of cell-cycle and apoptosis after exposure to ritonavir (Fig. 2). Ritonavir down-regulated the levels of survivin and cyclin D2 in EBV-immortalized B-cell lines. We also observed increased cleavage of PARP in these cells. However, ritonavir did not modulate the other regulators of cell-cycle and apoptosis such as Bcl-X_L, Bcl-2 and p53. Ritonavir had no effect on the expression of viral proteins such as LMP-1, suggesting that ritonavir may induce cell-cycle arrest and apoptosis by down-regulating the levels of survivin and cyclin D2 without reducing the virus levels in the cells.

Ritonavir suppresses constitutive NF-κB expressed by EBV-transformed LCLs

To examine the effect of ritonavir on NF-κB DNA binding, EMSA was performed. EBV-immortalized B-cell lines were incubated with or without 40 μM ritonavir for 24 h, and nuclear extracts were prepared and examined for NF-κB by EMSA.

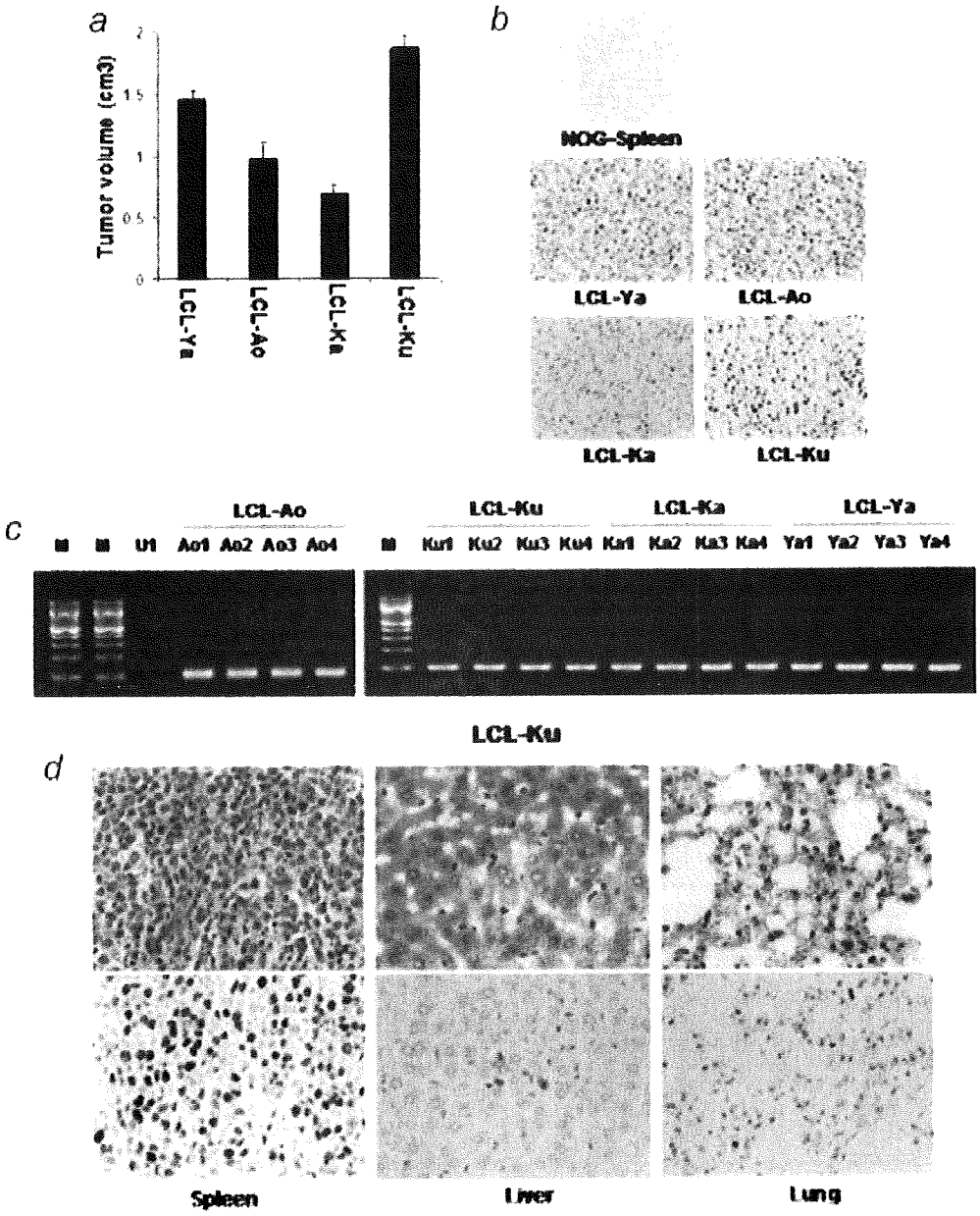

FIGURE 4 – Successful engraftment and infiltration of EBV-positive lymphoblastoid B cells in NOG mice. (*a*) Subcutaneous tumor size in mice 21 days after inoculation with various LCL cells. (*b*) *In situ* hybridization for EBER of spleen from NOG mice not receiving tumor cells, as a negative control and tumor tissues of LCL cells injected mice. Magnification ×40. (*c*) Detection of viral DNA by PCR. M, Marker; U1; EBV-negative U937 cell for negative control; Ao1, *in vitro* culture and Ao2, Ao3 and Ao4, *in vivo* samples from 3 different mice inoculated with LCL-Ao; Ku1, *in vitro* culture and Ku2, Ku3 and Ku4, *in vivo* sample from 3 different mice inoculated with LCL-Ku; Ka1, *in vitro* culture and Ka2, Ka3 and Ka4, *in vivo* sample from 3 different mice inoculated with LCL-Ka, Ya1, *in vitro* culture and Ya2, Ya3 and Ya4, *in vivo* sample from 3 different mice inoculated with. LCL-Ya. Infiltration of EBV-immortalized B-cell lines in various organs of NOG mice. (*d*) HE and *in situ* hybridization for EBER of spleen, liver and lung of mice inoculated with LCL-Ku cells. Left, middle and right panels represent spleen, liver and lung, respectively. Upper and lower panels represent HE and EBER, respectively (magnification ×40).

Down-regulation of NF-κB occurred in all cell lines (Fig. 3*a*, upper panels). Inhibition appeared specific to NF-κB, because no significant change in binding activity of AP-1 was observed after treatment of cells with ritonavir (Fig. 3*a*, lower panels). Also, the observed protein/DNA binding was specific for NF-κB, because the binding was effectively competed and abrogated by excess unlabeled NF-κB oligonucleotide but not by mutant NF-κB or AP-1 oligonucleotide (Fig. 3*b*). LCL-Ku cell extract without ritonavir treatment contained p50, p65 and Rel B proteins in the NF-κB complex (Fig. 3*b*, upper panel), and ritonavir did not affect components of the NF-κB complex (Fig. 3*b*, lower panel).

Efficient engraftment and infiltration of EBV-transformed LCLs in NOG mice

EBV-immortalized LCLs (LCL-Ya, LCL-Ao, LCL-Ka and LCL-Ku) were inoculated s.c. in the post-auricular region of NOG mice (Fig. 4 and Table I). Mice inoculated with LCL cells (LCL-

TABLE I – *IN VIVO* CHARATERISTICS OF EBV-POSITIVE LYMPHOBLASTOID B CELLS IN NOG MICE

Cell line	Orgin/EBV status	No. of cells inoculated/mouse (10^7)[1]	Inoculation route[2]	Day of sacrifice after inoculation	No. of mice with tumor/no. of mice inoculated[3]	Organ-infiltration[4]		
						Spleen	Liver	Lung
LCL-Ya	B/+	1	sc	21	03/03	++	–	–
LCL-Ao	B/+	1	sc	21	03/03	++	–	–
LCL-Ka	B/+	1	sc	21	03/03	++	–	–
LCL-Ku	B/+	1	sc	21	21/21	+++	+	+

[1]Mice were inoculated with 1×10^7 cells per mouse.–[2]sc, subcutaneous.–[3]Number of animals in which tumor developed.–[4]Organ-infiltration was examined by histological analysis.–, no infiltration; +, slight infiltration; ++, marked infiltration; +++, massive infiltration.

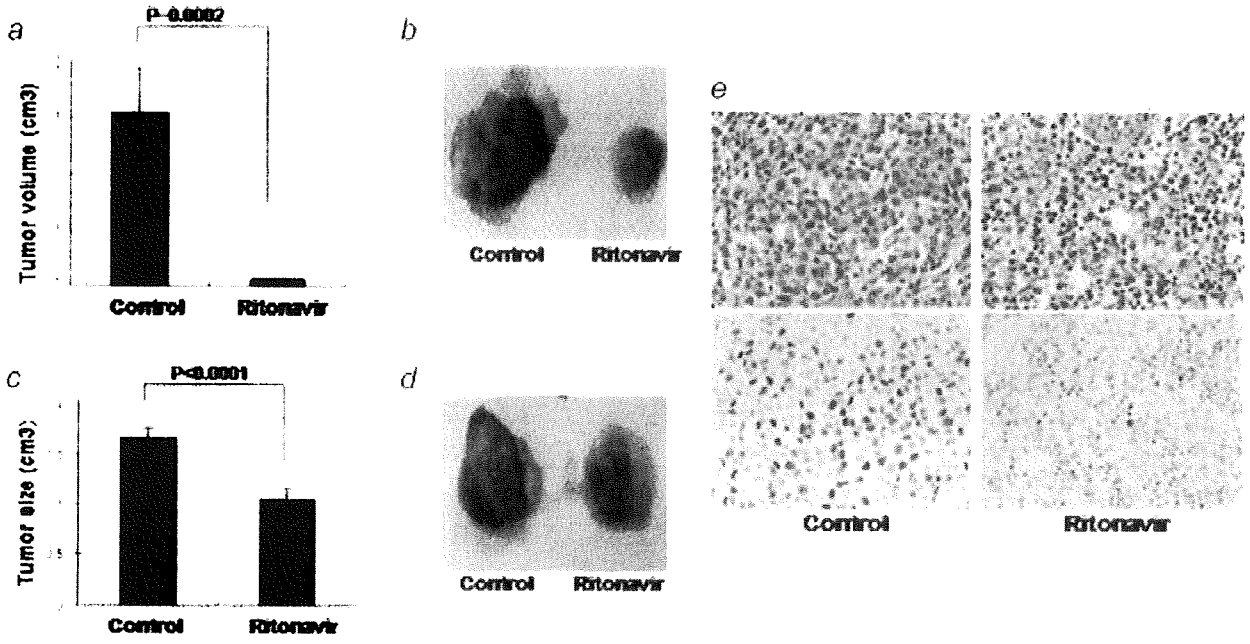

FIGURE 5 – Effect of ritonavir on lymphoma cell growth and infiltration. Mice were injected with LCL-Ku cells (1×10^7 cells) s.c. in the postauricular region. (*a* and *b*) The drug was administered s.c. into the tumor cells inoculated site of mice at doses of 30 mg/kg/day, beginning on day 0 for 3 weeks. The control mice received RPMI-1640 (200 µl) simultaneously. (*a*) Average size of tumor, data represent the mean ± SD from 6 mice. (*b*) Photograph of subcutaneously formed excised tumor without (left) and with (right) ritonavir treatment. (*c* and *d*) Effect of ritonavir on established tumor, ritonavir or RPMI-1640 was also administered intraperitoneally into mice as the same doses stated above, beginning on day 4 for 18 days. (*c*) Average size of tumor, data represent the mean ± SD from 6 mice. (*d*) Photograph of subcutaneously formed excised tumor without (left) and with (right) ritonavir treatment. (*e*) HE and *in situ* hybridization for EBER in spleen tissue of LCL cells injected mice. Magnification ×40. Upper and lower panels show HE and EBER staining, respectively.

Ya, LCL-Ao, LCL-Ka and LCL-Ku) produced a visible tumor within 3 weeks in all NOG mice. LCL-Ku cell was very efficient in the formation of a large tumor (Fig. 4*a*), as well as development of clinical signs of near-death, such as pilorection, weight loss and cachexia in mice at the time point of sacrifice. The average tumor size (LCL-Ya, LCL-Ao, LCL-Ka and LCL-Ku) in NOG mice inoculated s.c. with lymphoma cells was shown in Figure 4*a*. To test whether tumors maintain original histomorphology and expression patterns of tumor markers in NOG, we performed HE and *in situ* hybridization for EBER of normal mice spleen not receiving tumor cells and tumor tissues obtained from mice inoculated with LCLs. Histological analysis revealed that morphologically immunoblastic cells with large nucleus, clear nuclear membrane and broad cytoplasm expressed EBER, whereas EBER was not detected in spleen tissue collected from mice not receiving tumor cells, suggesting that *in vivo* tumor cells preserved well morphology as well as expressed viral gene EBER (Fig. 4*b*). Tumor cells from mice inoculated with EBV-immortalized B-cell lines were positive for DNA of EBV by PCR (Fig. 4*c*). These results showed that EBV-immortalized B-cell lines inoculated s.c. into the postauricular region of NOG mice were able to produce a visible tumor very efficiently. To assess the tissue distribution of lymphoma cells, we carried out histological examinations of the different organs of NOG mice after inoculation of the cells. Proliferation and infiltration of tumor cells were found not only in primary tumor tissues but also in spleen and to a lesser extent in liver and lung of NOG mice inoculated with tumor cells (Table I). HE and *in situ* hybridization staining for EBER showed a degree of infiltration of tumor cells at the site of inoculation and various organs with lymphoma cells (Fig. 4*d*). Interestingly, LCL-Ku cells appeared to infiltrate in various organs of mice more aggressively and massively than other cells. This extremely rapid tumor formation and infiltration in all mice is one of the hallmarks of our clinically relevant animal model without change of histomorphology or tumor marker expression.

Ritonavir suppresses the LCLs growth and infiltration in vivo

To determine the effect of ritonavir on tumor growth and infiltration, we injected LCL-Ku cells (1×10^7) s.c. into the postauricular region of NOG mice. Mice were treated with either RPMI-1640 (as control) or ritonavir (30 mg/kg/day), beginning on either day 0 or day 4. A significant decrease in the size of tumors in mice treated with ritonavir was demonstrated when compared with controls 3 weeks after the injection of tumor cells (Fig. 5*a*). Gross appearance of the mice treated by ritonavir showed apparent

reduction of the tumor mass at 3 weeks after inoculation of tumor cells (Fig. 5*b*). Ritonavir also inhibited the size and growth of established tumors (Fig. 5*c* and 5*d*). Ritonavir at this treatment dosage (30 mg/kg/day for 3 weeks) is well tolerated without adverse findings such as standing of hair, weight loss and cachexia of treated mice, all of which are signs of near death. Clinical evaluation of organ invasion 3 weeks after injection of tumor cells showed that ritonavir treatment inhibited their infiltration into spleen (Fig. 5*e*). In contrast, all control mice showed infiltration with tumor cells into spleen. Organ infiltration of lymphoma cells were analyzed and evaluated by HE and *in situ* hybridization of EBER. Together, these data indicate that ritonavir significantly inhibits lymphoma cell growth and infiltration in various organs of NOG mice (Fig. 5).These results suggest that ritonavir contributes to the reduction of the tumor growth and inhibits the organ infiltration in the mice through targeting the constitutive NF-κB activity.

Discussion

EBV-positive malignancies in immunocompromised patients are associated with high mortality and reduce overall survival period. The various chemotherapies so far developed have not increased significantly the survival of patients with EBV-associated malignancies in immunocompromised patients. Given disappointing results using conventional chemotherapy, new treatment strategies that specially target EBV-transformed cells are need.[1,2] LMP-1 is an oncogene that constitutively activates NF-κB to induce B cell proliferation.[7] It has been previously reported that suppression of high NF-κB activity inhibited cell growth and induced apoptosis of cancer cells as well as EBV-transformed cells both *in vitro* and *in vivo*.[12–20,33] Ritonavir is cytotoxic for different types of malignant cells *in vitro* through affecting proteasomal proteolysis, although concentrations necessary to show the *in vitro* effect exceed the achievable therapeutic drugs level.[27,29,30] It may affect the stabilization of p21, p27 and p53 proteins. Recently, ritonavir has been shown to inhibit NF-κB activity and induce the apoptosis of ATL cells.[20] This led us to investigate whether this drug exhibits anti-tumor effects against EBV-transformed cells *in vitro* and in our preclinical murine model. In the present study, we established a unique murine model that presents aggressive features concerning cell growth and infiltration in SCID mice within 3 weeks. Thus, it represents a novel model to evaluate tissue toxicity and the efficacy of therapeutic agents directed toward the treatment of EBV-associated lymphoproliferative diseases.

The blood-plasma ritonavir concentrations obtained in the therapy of HIV-infection are between 5 to 15 μM,[34] but much higher maximal concentrations (up to 46 μM) have been demonstrated in individual patients.[35] In the present study, we used the concentration of ritonavir for doing *in vitro* experiments from 0 to 40 μM and *in vivo* 30 mg/kg/day used for treatment of AIDS patients. Constitutive and strong NF-κB activation was reported to be a characteristic of LCL and important for LCL growth and survival.[7] Our results indicate that inhibition of NF-κB activity by ritonavir reduced cell growth and induced apoptosis of these cells. This is consistent with down-modulation of NF-κB regulated genes such as antiapoptotic and cell-cycle related genes. Our murine model clearly indicate that 30 mg/kg/day of ritonavir (the same dose used clinically for treating HIV/AIDS patients) significantly inhibits EBV-transformed cell growth and infiltration into various organs of NOG mice. The plasma exposure produced by this dose in mice is only approximately one-half of the plasma exposure observed with the licensed dose of ritonavir in human (600 mg BID). In our murine model, ritonavir at this treatment dosage is well tolerated without severe adverse effects observed in the mice during the treatment period. These data strongly suggest that the HIV protease inhibitor, ritonavir, is a promising antitumor agent against EBV-transformed cells and could be used clinically for treatment of EBV-associated malignancies. These results suggest that anti-tumor activity of ritonavir correlates with suppression of NF-κB activity.

In summary, we have established a novel NOG EBV-associated lymphoma model that presents features similar to patients with EBV-infection in immunocompromised patients. These results also indicate that the HIV protease inhibitor, ritonavir, showed antitumor and anti-NF-κB activity against EBV-transformed cells. Finally, our results strongly suggest that NF-κB serves as a potential molecular target to treat EBV-associated malignancies, and that ritonavir might be used clinically as a single compound or in combination with the reducing dose of chemotherapeutic agents for treatment of patients with life-threatening EBV-associated lymphoproliferative diseases and AIDS-associated lymphomas.

Acknowledgements

We thank D. Kempf and T. Yamada of Abbott Laboratories, S. Ichinose of Instrumental Analysis Research Center and S. Endo of Animal Research Center, Tokyo Medical and Dental University for their advice and assistance with the experiments. We also thank Y. Sato of the National Institute of Infectious Diseases for her excellent technical assistance.

References

1. Rickinson AB, Kieff E. Epstein-Barr virus. In: Fields BN, ed. Fields virology, 4th edn. New York (NY): Lippincott Williams and Wilkins, 2001. Vol. 1, 2575–627.
2. Kieff E, Rickinson AB. Epstein-Barr virus and replication. In: Fields BN, ed. Fields virology, 4th ed. New York (NY): Lippincott Williams and Wilkins, 2001. Vol. 1, 2511–73.
3. Zur Hausen H, Schulte-Holthausen H. Presence of EB virus nucleic acid homology in a "virus-free" line of Burkitt tumour cells. Nature 1970;227:245–48.
4. Nonoyama M, Pagano JS. Homology between Epstein-Barr virus DNA and viral DNA from Burkitt's lymphoma and nasopharyngeal carcinoma determined by DNA-DNA reassociation kinetics. Nature 1973;242:44–7.
5. Rowe M, Lear AL, Croom-Carter D, Davies AH, Rickinson AB. Three pathways of Epstein-Barr virus gene activation from EBNA1-positive latency in B lymphocytes. J Virol 1992;66:122–31.
6. Yamamoto N, Takizawa T, Iwanaga Y, Shimizu N, Yamamoto N. Malignant transformation of B lymphoma cell line BJAB by Epstein-Barr virus-encoded small RNAs. FEBS Lett 2000;484:153–58.
7. Mosialos G, Birkenbach M, Yalamanchili R, VanArsdale T, Ware C, Kieff E. The Epstein-Barr virus transforming protein LMP1 engages signaling proteins for the tumor necrosis factor receptor family. Cell 1995;80:389–99.
8. Mori N, Fujii M, Ikeda S, Yamada Y, Tomonaga M, Ballard DW, Yamamoto N. Constitutive activation of NF-κB in primary adult T-cell leukemia cells. Blood 1999;93:2360–8.
9. Baldwin AS. The NF-κB and IκB proteins: new discoveries and insights. Annu Rev Immunol 1999;14:649–81.
10. Guinness ME, Kenney JL, Reiss M, Lacy J. Bcl-2 antisense oligodeoxynucleotide therapy of Epstein-Barr virus-associated lymphoproliferative disease in severe combined immunodeficient mice. Cancer Res 2000;60:5354–8.
11. Miyake A, Dewan MZ, Ishida T, Watanabe M, Honda M, Sata T, Yamamoto N, Umezawa K, Watanabe T, Horie R. Induction of apoptosis in Epstein-Barr virus-infected B-lymphocytes by the NF-kappaB inhibitor DHMEQ. Microbes Infect 2008;10:748–56.
12. Watanabe M, Dewan MZ, Okamura T, Sasaki M, Itoh K, Higashihara M, Mizoguchi H, Honda M, Sata T, Watanabe T, Yamamoto N, Umezawa K, et al. A novel NF-κB inhibitor DHMEQ selectively targets constitutive NF-κB activity and induces apoptosis of multiple myeloma cells in vitro and in vivo. Int J Cancer 2005;114:32–8.
13. Adams J, Palombella VJ, Elliott PJ. Proteasome inhibition: a new strategy in cancer treatment. Invest New Drugs 2001;18:109–21.
14. Teicher BA, Ara G, Herbst R, Palombella VJ, Adams J. The proteasome inhibitor PS-341 in cancer therapy. Clin Cancer Res 1999; 5:2638–45.